

Article

# Mathematical and Stability Analysis of Dengue–Malaria Co-Infection with Disease Control Strategies

Azhar Iqbal Kashif Butt <sup>1,\*</sup>, Muhammad Imran <sup>2,\*</sup>, Brett A. McKinney <sup>2,†</sup>, Saira Batool <sup>2,3,†</sup> and Hassan Aftab <sup>4,†</sup>

<sup>1</sup> Department of Mathematics and Statistics, College of Science, King Faisal University, Al-Ahsa 31982, Saudi Arabia

<sup>2</sup> Tandy School of Computer Science, University of Tulsa, Tulsa, OK 74104, USA; brett-mckinney@utulsa.edu (B.A.M.); batoolsaira991@gmail.com (S.B.)

<sup>3</sup> Department of Mathematics, Government Associate College (W) Kamar Mashani, Mianwali 42400, Pakistan

<sup>4</sup> Department of Mathematics, COMSATS University Islamabad, Lahore Campus, Lahore 54000, Pakistan; hassanaftab.ha501@gmail.com

\* Correspondence: aikhan@kfu.edu.sa (A.I.K.B.); mui7451@utulsa.edu (M.I.)

† These authors contributed equally to this work.

**Abstract:** Historically, humans have been infected by mosquito-borne diseases, including dengue fever and malaria fever. There is an urgent need for comprehensive methods in the prevention, control, and awareness of the hazards posed by dengue and malaria fever to public health. We propose a new mathematical model for dengue and malaria co-infection with the aim of comprehending disease dynamics better and developing more efficient control strategies in light of the threat posed to public health by co-infection. The proposed mathematical model comprises four time-dependent vector population classes ( $S\mathcal{E}I_dI_m$ ) and seven host population classes ( $S\mathcal{E}I_dI_mI_{dm}TR$ ). First, we show that the proposed model is well defined by proving that it is bounded and positive in a feasible region. We further identify the equilibrium states of the model, including disease-free and endemic equilibrium points, where we perform stability analysis at equilibrium points. Then, we determine the reproduction number  $R_0$  to measure the level of disease containment. We perform a sensitivity analysis of the model's parameters to identify the most critical ones for potential control strategies. We also prove that the proposed model is well posed. Finally, the article examines three distinct co-infection control measures, including spraying or killing vectors, taking precautions for one's own safety, and reducing the infectious contact between the host and vector populations. The control analysis of the proposed model reveals that all control parameters are effective in disease control. However, self-precaution is the most effective and accessible method, and the reduction of the vector population through spraying is the second most effective strategy to implement. Disease eradication is attainable as the vector population decreases. The effectiveness of the implemented strategies is also illustrated with the help of graphs.

**Keywords:** mathematical model; dengue–malaria co-infection; stability analysis; sensitivity analysis; control analysis

**MSC:** 34H05; 49K15; 65K10



**Citation:** Butt, A.I.K.; Imran, M.; McKinney, B.A.; Batool, S.; Aftab, H. Mathematical and Stability Analysis of Dengue–Malaria Co-Infection with Disease Control Strategies. *Mathematics* **2023**, *11*, 4600. <https://doi.org/10.3390/math11224600>

Academic Editors: Osman Tunc, Vitalii Slynko and Sandra Pinelas

Received: 3 October 2023

Revised: 4 November 2023

Accepted: 7 November 2023

Published: 9 November 2023



**Copyright:** © 2023 by the authors. Licensee MDPI, Basel, Switzerland. This article is an open access article distributed under the terms and conditions of the Creative Commons Attribution (CC BY) license (<https://creativecommons.org/licenses/by/4.0/>).

## 1. Introduction

Dengue fever is a dangerous vector-borne disease. The disease-causing dengue virus is transmitted through the bites of female *Aedes* mosquitoes, as documented in various sources [1–3]. When a mosquito bites an infectious human, the dengue virus moves from the human into the mosquito's bloodstream. Subsequently, when the same mosquito bites a healthy human, the dengue virus is transmitted to the new host [4,5]. A 2012 report indicates that more than a hundred countries worldwide have a population at risk of

contracting dengue fever [6,7]. In recent years, there have been several outbreaks of dengue infections in various countries that have caused significant harm to society [8–11]. Dengue fever can cause the destruction of white blood cells and a rapid decrease in platelet count, as noted in Ref. [12]. Other symptoms of dengue fever include high fever, vomiting, abdominal pain or tenderness, persistent vomiting, clinical fluid accumulation, mucosal bleeding, lethargy, and liver enlargement [13].

The malaria disease is caused by the plasmodium parasite and is transmitted through female anopheles mosquitoes to humans, as stated by the World Health Organization (WHO) [14]. Malaria has a more dangerous and ancient history than other mosquito-borne diseases like dengue. According to the WHO malaria report, the number of malaria cases increased from 216 million in 2016 to 320 million in 2017 [15,16] and reported around 241 million malaria cases globally, with 627,000 malaria deaths predicted in 2020 [17]. Africa was the dominant region in 2020, with 95% of malaria cases and 96% of malaria deaths [17,18]. In that location, 80% of the total casualties were youngsters under the age of five. Despite decades of global eradication and control attempts, the disease has resurfaced in locations where control measures were previously effective [18]. The common symptoms of malaria include fever, sweating, shivering or cold, vomiting, headache, diarrhea, and muscle aches. The latent period of malaria lasts from 7 to 14 days [14–19].

The diseases dengue and malaria share the same vector (mosquito) and have similar initial symptoms, making it possible for a person to be affected by both at the same time [20–25]. Dengue fever and malaria are comparable in terms of transmission and impact on human health. Both illnesses are vector-borne, which means they are spread to people via the bites of infected mosquitoes. Mosquitoes of some species serve as carriers for the viruses that cause dengue fever and the parasites that cause malaria. Furthermore, these illnesses have been present throughout human history, impacting communities all over the world. Both dengue and malaria can cause high fevers, lethargy, and body pains, causing severe suffering for those who are infected. Furthermore, if left undiagnosed or poorly managed, these illnesses can cause serious consequences and, in extreme situations, even death. In light of the fact that these two diseases have a number of similarities in common, it is of the utmost importance to give priority to implementation of comprehensive preventive and control measures in order to successfully combat the spread of both dengue and malaria. As highlighted in [20], the documented instances of dengue–malaria co-infection in 2016 were 26 in India, 4 in Pakistan, 1 in Cambodia, 1 in Malaysia, 1 in Bangladesh, 1 in Japan, and 1 in East Timor. Taking into account these facts, we will develop a comprehensive mathematical model to effectively capture the complexities of dengue and malaria dynamics, while also addressing the occurrence of co-infection of these two diseases. This model will also provide a solid foundation for practical and reliable analysis.

Mathematical modeling is a highly reliable and effective tool for understanding biological and physical problems, and patterns [26–29]. In the domain of epidemiology, mathematical models have played a crucial role in understanding the disease transmission dynamics for disease control and analysis [30–32]. By combining mathematical techniques with epidemiological knowledge, researchers can simulate various scenarios, explore different interventions, and guide public health decision making [33–35]. The foundation of epidemiological models can be traced back to Kermack and McKendrick [36], who developed the deterministic SIR epidemic model in 1927 and later expanded it to SEIR. Over time, numerous mathematical models have been proposed in the literature for various diseases, e.g., coronavirus, tuberculosis, whooping cough, and lumpy skin disease [37–39].

In [6], the authors developed a modified SEIR host population and SI vector population fractional-order model for dengue dynamics, incorporating the well-known Atangana Baleanu Caputo derivative in the Caputo sense. The authors introduced additional compartments in the host population, namely the treatment compartment and the protected traveler's compartment, and formulated an optimal control problem using treatment as the control variable. Similarly, in [7], the authors proposed an SEIHR dengue model with optimal

control for real-world data, demonstrating the significance of the proposed model and control strategies. The authors in [8] introduced a mathematical model based on the Caputo fractional calculus. This model partitions the overall human population into four distinct compartments, namely susceptible, infected (both symptomatic and carriers), partially immunized individuals, and the recovered class. Likewise, the total vector population is categorized into susceptible and infected groups. The authors demonstrated and substantiated the fundamental characteristics of the proposed epidemic model utilizing Caputo fractional derivatives. Additionally, they highlighted the benefits associated with fractional derivatives, such as the incorporation of memory effects.

Various mathematical models exist for malaria as well, each based on different assumptions and control strategies, such as those presented in [15–17]. In [15], the focus was on mathematical modeling and two control strategies: human precautions and mosquito sprays. Both strategies exert a noteworthy influence on disease control; however, self-precaution emerges as the more efficacious approach. The system attains a disease-free state when a minimum of 40% of susceptible humans undertake the requisite precautions. Similarly, in [17], the authors presented an effective control approach called awareness-based intervention employing media for malaria management. Their mathematical model evaluates interventions (e.g., mosquito nets) and includes a dynamic awareness variable. This model categorizes people by awareness, considering shifts from awareness to unawareness, connecting recovery to awareness-dependent treatments. The model features time-dependent control functions for treatment, insecticides, and social media campaigns, aiming to minimize malaria control costs. In Ref. [19], the authors developed a new mathematical model for malaria using partial differential equations, dividing vector and host populations into distinct compartments. They investigated the effectiveness of spraying in malaria control, utilizing both classical and impulsive methods. Their findings suggested that uniform spraying yielded results comparable to a non-spatial model.

Limited articles are available in the existing literature that focus on the co-infection of dengue and malaria. One notable instance is found in [20], where an exhaustive and comprehensive examination of dengue–malaria co-infection is presented. This study encompassed a thorough exploration of clinical manifestations and diagnostic challenges associated with the co-infection. Similarly, in another study, the authors shed light on the particulars of the initial instance of dengue–malaria co-infection documented in Nepal [23]. Both of these articles contribute to a broader understanding of dengue–malaria co-infection by offering comprehensive case studies. The mathematical model for co-infection between malaria and dengue is represented by a deterministic system of non-linear ODEs in [25]. The authors proposed a deterministic model for dengue and malaria co-infection that deals with two submodels, dengue only and malaria only, and then combines them into a dengue and malaria co-infection model. The purpose of the proposed mathematical model is to provide a brief introduction to the disease as well as the stability analysis of the proposed model through analytical and numerical methods. The article is basic and comprehensive for the motivation of epidemiologists, but it covers a very short area of the field, and more work can be conducted, e.g., sensitivity and control analysis. However, no article currently provides comprehensive insight, detailed analysis, and valuable control strategies specifically for the co-infection of dengue and malaria. To fill these gaps in the literature, we proposed an extended mathematical model for the dengue–malaria co-infection.

In the current manuscript, we present a mathematical model for dengue–malaria fever, which is a vector-borne disease. We divide the total vector population  $\mathcal{N}$  into four sub-compartments, including susceptible mosquitoes  $\mathcal{S}$ , exposed mosquitoes  $\mathcal{E}$ , dengue-infectious mosquitoes  $\mathcal{I}_d$ , and malaria-infectious mosquitoes  $\mathcal{I}_m$ . Similarly, the human population  $\mathbb{N}$  is divided into seven sub-departments, including susceptible humans  $\mathbb{S}$ , exposed humans  $\mathbb{E}$ , dengue-infectious humans  $\mathbb{I}_d$ , malaria-infectious humans  $\mathbb{I}_m$ , dengue–malaria-infectious humans  $\mathbb{I}_{dm}$ , under-treatment humans  $\mathbb{T}$ , and recovered humans  $\mathbb{R}$ . We assume that the susceptible populations, both vector and host, are non-infectious and can contract the virus from infectious populations. The exposed class includes both types

of viruses and remains exposed before identification of symptoms.  $\mathcal{I}_d$  and  $\mathbb{I}_d$  represent dengue-infectious vector and dengue-infectious human, respectively. Similarly,  $\mathcal{I}_m$  and  $\mathbb{I}_m$  represent malaria-infectious vector and malaria-infectious human, respectively. We also introduce a dengue–malaria-infectious human class, represented by  $\mathbb{I}_{dm}$ , for people who have both diseases at the same time. All treatments or precautions taken by infectious humans at home or in the hospital to reduce the effects of dengue, malaria, and dengue–malaria co-infection are represented by  $\mathbb{T}$ . Finally, the recovered or removed people are categorized as  $\mathbb{R}$ . The transmission rates, which vary from compartment to compartment, are given in Table 1 along with their descriptions, values and references. The main purpose of constructing such a model is to understand the transmission dynamics of the dengue–malaria co-infection in order to propose a reliable and comprehensive control strategy.

**Table 1.** Parametric description and the corresponding values.

Parameter	Description	Value	Source
$\Pi$	Recruitment rate of mosquito	3839.9	[7]
$\nu$	Natural death rate of mosquito	0.05244	Assumed
$\Phi_1$	Interaction rate of $\mathcal{S}$ and $\mathbb{I}_d$	$1.197 \times 0.8541$	[7]
$\Phi_2$	Interaction rate of $\mathcal{S}$ and $\mathbb{I}_m$	0.729255	[15]
$\Phi_3$	Interaction rate of $\mathcal{S}$ and $\mathbb{I}_{dm}$	0.00002181	Assumed
$\Phi_4$	Translation from $\mathcal{E}$ to $\mathcal{I}_d$	0.7186	[7]
$\Phi_5$	Translation from $\mathcal{E}$ to $\mathcal{I}_m$	0.291499	[15]
$\Psi$	Recruitment rate of humans	1525.1426	[7]
$\mu$	Natural death rate of humans	$1/(70.97 \times 365)$	[7]
$\beta_1$	Interaction rate of $\mathbb{S}$ and $\mathcal{I}_d$	$0.01971 \times 0.06794$	[7]
$\alpha_1$	Interaction rate of $\mathbb{S}$ and $\mathcal{I}_m$	0.5837773	[15]
$\beta_2$	Translation from $\mathbb{E}$ to $\mathbb{I}_d$	0.0555	[7]
$\alpha_2$	Translation from $\mathbb{E}$ to $\mathbb{I}_m$	0.0140705	[15]
$\gamma_1$	Translation from $\mathbb{E}$ to $\mathbb{I}_{dm}$	0.02	Assumed
$\beta_3$	Medication rate of $\mathbb{I}_d$	0.0904	[7]
$\alpha_3$	Medication rate of $\mathbb{I}_m$	0.01325	Assumed
$\gamma_2$	Medication rate of $\mathbb{I}_{dm}$	0.02	Assumed
$\gamma_3$	Recovery rate of $\mathbb{T}$	0.0840	[7]
$\delta_{\mathbb{I}_d}$	Dengue induced mortality of $\mathbb{I}_d$	0.08	Assumed
$\delta_{\mathbb{I}_m}$	Malaria induced mortality of $\mathbb{I}_m$	0.08	Assumed
$\delta_{\mathbb{I}_{dm}}$	Dengue–malaria induced mortality of $\mathbb{I}_{dm}$	0.1	Assumed
$\delta_{\mathbb{T}}$	Disease induced mortality of $\mathbb{T}$	0.05	Assumed

This paper is organized as follows: Section 2 discusses the formulation of the dengue–malaria co-infection model. Section 3 deals with the fundamental properties of the solution, e.g., the existence of uniqueness and positive bounded solution. Section 4 of the paper analyzes the equilibrium points and reproduction number ( $R_0$ ), while Section 5 discusses the local and global asymptotic stability of both the disease-free and endemic equilibrium points. In Section 6, a comprehensive sensitivity analysis of the reproduction number to parameters is carried out. The paper then addresses various controls with different levels of control values in Section 7, and numerical simulations are also presented in this section. Finally, Section 8 summarizes the findings of the manuscript.

### 2. Formulation of Dengue–Malaria Model

We classify the overall population of vectors and hosts as  $\mathcal{N}(t)$  and  $\mathbb{N}(t)$ , respectively, into four and seven time-dependent classes. The vector population is divided into susceptible  $\mathcal{S}(t)$ , exposed  $\mathcal{E}(t)$ , dengue-infectious  $\mathcal{I}_d(t)$ , and malaria-infectious  $\mathcal{I}_m(t)$  categories. Therefore, the complete vector population  $\mathcal{N}(t)$  at any given time  $t$  can be expressed as:

$$\mathcal{N}(t) = \mathcal{S}(t) + \mathcal{E}(t) + \mathcal{I}_d(t) + \mathcal{I}_m(t). \tag{1}$$

Assuming that the recruitment and death rates of susceptible vectors are  $\Pi$  and  $\nu$ , respectively, the mosquitoes become exposed by biting infectious humans at the rates of  $\Phi_1$ ,  $\Phi_2$ , and  $\Phi_3$ . The exposed mosquitoes are then converted to dengue-infectious and malaria-infectious vectors at rates of  $\Phi_4$  and  $\Phi_5$ , respectively. Under these assumptions, we obtain the following system of differential equations:

$$\frac{dS}{dt} = \Pi - \frac{(\Phi_1 I_d + \Phi_2 I_m + \Phi_3 I_{dm})S}{N} - \nu S, \tag{2a}$$

$$\frac{dE}{dt} = \frac{(\Phi_1 I_d + \Phi_2 I_m + \Phi_3 I_{dm})S}{N} - (\Phi_4 + \Phi_5 + \nu)E, \tag{2b}$$

$$\frac{dI_d}{dt} = \Phi_4 E - \nu I_d, \tag{2c}$$

$$\frac{dI_m}{dt} = \Phi_5 E - \nu I_m, \tag{2d}$$

with non-negative initial conditions:

$$S(0) = S_0 > 0, \quad E(0) = E_0 \geq 0, \quad I_d(0) = I_{d0} \geq 0, \quad I_m(0) = I_{m0} \geq 0. \tag{2e}$$

As mentioned above, the total host population  $N(t)$  is divided into seven classes. The first host class is given as the susceptible  $S(t)$  class. In this class, we take those individuals who are at risk and can be infected after being bitten by one or both types of infectious mosquitoes. After the biting of mosquitoes, the susceptible people become exposed  $E(t)$ . During the latent period, the host does not show any symptoms of dengue or malaria. After the latent period, a host patient may get an infection from dengue, malaria, or both at the same time. Therefore, exposure may move to dengue-infectious  $I_d(t)$ , malaria-infectious  $I_m(t)$  and both dengue–malaria-infectious  $I_{dm}(t)$  compartments. It also assumes that infectious humans who are receiving treatment at home or in a hospital are taken in  $T(t)$ . In the end, recovered or removed are taken in  $R(t)$ . Hence, the total host population, denoted by  $N(t)$ , is given by:

$$N(t) = S(t) + E(t) + I_d(t) + I_m(t) + I_{dm}(t) + T(t) + R(t). \tag{3}$$

We assume that  $\Psi$  and  $\mu$  represent the recruitment and natural death rates of the host population, respectively, and  $\beta_i$ ,  $\alpha_i$  and  $\gamma_i$ ,  $i = 1, 2, 3$  represent the transmission and translations within the host populations. The values and complete description of the parameters are given in Table 1.

Under the above-mentioned assumptions and considerations, the mathematical model of the host population is given by the following system of differential equations.

$$\frac{dS}{dt} = \Psi - \frac{(\beta_1 I_d + \alpha_1 I_m)S}{N} - \mu S, \tag{4a}$$

$$\frac{dE}{dt} = \frac{(\beta_1 I_d + \alpha_1 I_m)S}{N} - (\beta_2 + \alpha_2 + \gamma_1 + \mu)E, \tag{4b}$$

$$\frac{dI_d}{dt} = \beta_2 E - (\beta_3 + \mu + \delta_{I_d})I_d, \tag{4c}$$

$$\frac{dI_m}{dt} = \alpha_2 E - (\alpha_3 + \mu + \delta_{I_m})I_m, \tag{4d}$$

$$\frac{dI_{dm}}{dt} = \gamma_1 E - (\gamma_2 + \mu + \delta_{I_{dm}})I_{dm}, \tag{4e}$$

$$\frac{dT}{dt} = \beta_3 I_d + \alpha_3 I_m + \gamma_2 I_{dm} - (\gamma_3 + \mu + \delta_T)T, \tag{4f}$$

$$\frac{dR}{dt} = \gamma_3 T - \mu R, \tag{4g}$$

with non-negative initial conditions:

$$\begin{aligned}
 S(0) = S_0 > 0, E(0) = E_0 \geq 0, I_d(0) = I_{d0} \geq 0, I_m(0) = I_{m0} \geq 0, \\
 I_{dm}(0) = I_{dm0} \geq 0, T(0) = T_0 \geq 0, R(0) = R_0 \geq 0.
 \end{aligned}
 \tag{4h}$$

A flow diagram of dengue–malaria co-infection is given in Figure 1. From this figure, we write the following system of non-linear ODEs that describe the dynamics of the dengue–malaria co-infection.

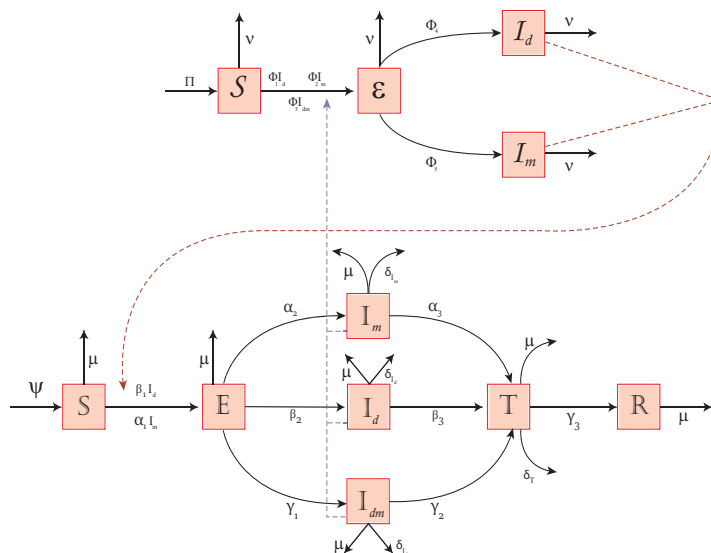


**Figure 1.** The flow diagram for dengue–malaria co-infection visually shows how the diseases spread. Pink and blue lines depict mosquito bites on healthy and infected humans. Black lines show how the mosquito and host populations move between compartments.

$$\frac{dS}{dt} = \Pi - \frac{(\Phi_1 I_d + \Phi_2 I_m + \Phi_3 I_{dm})S}{N} - \nu S,
 \tag{5a}$$

$$\frac{dE}{dt} = \frac{(\Phi_1 I_d + \Phi_2 I_m + \Phi_3 I_{dm})S}{N} - (\Phi_4 + \Phi_5 + \nu)E,
 \tag{5b}$$

$$\frac{dI_d}{dt} = \Phi_4 E - \nu I_d,
 \tag{5c}$$

$$\frac{dI_m}{dt} = \Phi_5 E - \nu I_m,
 \tag{5d}$$

$$\frac{dS}{dt} = \Psi - \frac{(\beta_1 I_d + \alpha_1 I_m)S}{N} - \mu S,
 \tag{5e}$$

$$\frac{dE}{dt} = \frac{(\beta_1 I_d + \alpha_1 I_m)S}{N} - (\beta_2 + \alpha_2 + \gamma_1 + \mu)E,
 \tag{5f}$$

$$\frac{dI_d}{dt} = \beta_2 E - (\beta_3 + \mu + \delta_{I_d})I_d,
 \tag{5g}$$

$$\frac{dI_m}{dt} = \alpha_2 E - (\alpha_3 + \mu + \delta_{I_m})I_m,
 \tag{5h}$$

$$\frac{dI_{dm}}{dt} = \gamma_1 E - (\gamma_2 + \mu + \delta_{I_{dm}})I_{dm},
 \tag{5i}$$

$$\frac{dT}{dt} = \beta_3 I_d + \alpha_3 I_m + \gamma_2 I_{dm} - (\gamma_3 + \mu + \delta_T)T,
 \tag{5j}$$

$$\frac{dR}{dt} = \gamma_3 T - \mu R,
 \tag{5k}$$

with non-negative initial conditions:

$$\begin{aligned} \mathcal{S}(0) = \mathcal{S}_0 > 0, \mathcal{E}(0) = \mathcal{E}_0 \geq 0, \mathcal{I}_d(0) = \mathcal{I}_{d0} \geq 0, \mathcal{I}_m(0) = \mathcal{I}_{m0} \geq 0, \\ \mathbb{S}(0) = \mathbb{S}_0 > 0, \mathbb{E}(0) = \mathbb{E}_0 \geq 0, \mathbb{I}_d(0) = \mathbb{I}_{d0} \geq 0, \mathbb{I}_m(0) = \mathbb{I}_{m0} \geq 0, \\ \mathbb{I}_{dm}(0) = \mathbb{I}_{dm0} \geq 0, \mathbb{T}(0) = \mathbb{T}_0 \geq 0, \mathbb{R}(0) = \mathbb{R}_0. \end{aligned} \tag{51}$$

### 3. Theoretical Properties of the Dengue–Malaria Co-Infection Model

In this section, we will prove the essential properties of the proposed mathematical model (5), e.g., the existence of a unique solution and feasible region for the system solution.

#### 3.1. Existence of a Unique Solution

Model (5) can be re-written as

$$\dot{x}(t) = G(t, x(t)), x(0) = x_0 \geq 0, \tag{6}$$

where  $G(t, x)$  represent the compact form of the right-hand sides of equations of Model (5),  $x(t) = (\mathcal{S}, \mathcal{E}, \mathcal{I}_d, \mathcal{I}_m, \mathbb{S}, \mathbb{E}, \mathbb{I}_d, \mathbb{I}_m, \mathbb{I}_{dm}, \mathbb{T}, \mathbb{R})^T \in \mathbb{R}^{11}$ , and  $x_0(t) = (\mathcal{S}_0, \mathcal{E}_0, \mathcal{I}_{d0}, \mathcal{I}_{m0}, \mathbb{S}_0, \mathbb{E}_0, \mathbb{I}_{d0}, \mathbb{I}_{m0}, \mathbb{I}_{dm0}, \mathbb{T}_0, \mathbb{R}_0)^T$  is the initial vector. Now, to prove the existence of the unique solution of (5), it is enough to prove that (6) has a unique solution. We will prove the existence of a unique solution by using fundamental and well-known results of calculus and functional analysis.

**Definition 1 (Picard Mapping [40]).** Given a point  $(t_0, z_0) \in R \times R^n$  and a differential equation

$$\frac{dz}{dt} = h(t, z),$$

where  $z \in R^n$  and  $h$  is a vector field over  $R \times R^n$ , identify the Picard mapping towards mapping  $\psi$  that takes a function  $\phi : t \rightarrow z$  to the function  $\psi\phi : t \rightarrow z$ , such as

$$(\psi\phi)(t) = z_0 + \int_{t_0}^t h(\tau, \phi(\tau))d\tau,$$

with

$$(\psi\phi)(t_0) = z_0.$$

**Theorem 1 ([40]).** The mapping  $\phi : R \rightarrow R^n$  is a solution to

$$\frac{dz}{dt} = h(t, z),$$

with initial condition

$$\phi(t_0) = z_0,$$

if and only if

$$\psi\phi = \phi,$$

where

$$(\psi\phi)(t) = z_0 + \int_{t_0}^t h(\tau, \phi(\tau))d\tau,$$

with

$$(\psi\phi)(t_0) = z_0.$$

**Theorem 2.** The right-hand-side function  $G(t, x(t))$  of (6) is Lipschitz continuous in the second argument  $x$  if  $G(t, x(t)) \in C^1[0, T_f]$ .

**Proof.** Let  $S$  be a convex compact subset of

$$X = \{(t, x(t)) \mid 0 \leq t \leq T_f, x(t) \in \mathbb{R}^{11}\}.$$

Let  $(t, \hat{x}(t)), (t, \tilde{x}(t)) \in S$ , then by the mean value theorem for differentiation  $\exists \zeta(t) \in (\hat{x}(t), \tilde{x}(t))$  such that

$$\frac{G(t, \hat{x}(t)) - G(t, \tilde{x}(t))}{\hat{x}(t) - \tilde{x}(t)} = G'(t, \zeta(t)),$$

where

$$G'(t, \zeta(t)) = \sum_{i=1}^7 \frac{\partial G(t, \zeta(t))}{\partial x_i}.$$

Hence,

$$G(t, \hat{x}(t)) - G(t, \tilde{x}(t)) = G'(t, \zeta(t)) \cdot (\hat{x}(t) - \tilde{x}(t)).$$

$$\begin{aligned} |G(t, \hat{x}(t)) - G(t, \tilde{x}(t))| &= |G'(t, \zeta(t)) \cdot (\hat{x}(t) - \tilde{x}(t))|, \\ &\leq \|G'(t, \zeta(t))\| \|(\hat{x}(t) - \tilde{x}(t))\|. \end{aligned}$$

Since  $G \in C^1[0, T_f]$ , over convex compact set  $S$ ,  $\exists \beta > 0$  such that

$$\|G'(t, \zeta(t))\| \leq \beta,$$

hence,

$$\begin{aligned} |G(t, \hat{x}(t)) - G(t, \tilde{x}(t))| &\leq \beta \|(\hat{x}(t) - \tilde{x}(t))\|, \\ \sup_{t \in [0, T_f]} |G(t, \hat{x}(t)) - G(t, \tilde{x}(t))| &\leq \beta \sup_{t \in [0, T_f]} \|(\hat{x}(t) - \tilde{x}(t))\|, \\ \|G(t, \hat{x}(t)) - G(t, \tilde{x}(t))\| &\leq \beta \|\hat{x}(t) - \tilde{x}(t)\|. \end{aligned}$$

Hence,  $G(t, x(t))$  is Lipschitz in the second argument.  $\square$

**Lemma 1** ([41]). Let  $T : X \rightarrow X$  be a continuous mapping on a complete metric space  $X = (X, d)$ , and suppose that  $T^m$  is a contraction on  $X$  for some positive integer  $m$ . Then,  $T$  has a unique fixed point.

**Theorem 3.** The solution of (6) exists and is unique provided  $G(t, x(t))$  is Lipschitz continuous and  $0 < T_f \beta < 1$ .

**Proof.** According to the Picard fixed-point theorem 1, any solution  $x(t)$  of (6) exist if it is the fixed point of the Picard mapping. Therefore, the solution will satisfy the following equation:

$$x(t) = (\psi x)(t) = x_0 + \int_0^t G(\tau, x(\tau)) d\tau, \text{ along with } (\psi x)(t_0) = x_0. \tag{7}$$

Let  $x(t)$  be a solution of (6). Then, by the fundamental theorem of calculus (FTOC),  $G(t, x(t))$  is continuous and hence integrable. Applying the integral on both sides of (6), we obtain

$$x(t) = x_0 + \int_0^t G(\tau, x(\tau)) d\tau,$$

which is equivalent to (7); hence,  $x(t)$  is the fixed point of the Picard mapping. Now for inverse implication, we define a Picard mapping  $\psi$  and will show that  $x(t)$  is the fixed point of this mapping. Let the Picard mapping  $\psi$ , define as

$$(\psi x)(t) = x_0 + \int_0^t G(\tau, x(\tau))d\tau, \quad (\psi x)(0) = x_0.$$

By Lemma 1, the Picard mapping  $\psi$  has a unique fixed point if the mapping is a contraction. Let  $x_1(t)$  and  $x_2(t) \in R^{11}$ , then

$$\begin{aligned} d(\psi(x_1), \psi(x_2)) &= \sup_{\tau \in [0, T_f]} \left| \int_0^{\tau} G(\tau, x_1(\tau))d\tau - \int_0^{\tau} G(\tau, x_2(\tau))d\tau \right| \\ &\leq \int_0^{T_f} \sup_{\tau \in [0, T_f]} |G(\tau, x_1(\tau)) - G(\tau, x_2(\tau))|d\tau. \end{aligned}$$

Since  $G(\tau, x(\tau))$  is Lipchitz in the second argument,

$$\begin{aligned} d(\psi(x_1), \psi(x_2)) &\leq \int_0^{T_f} \beta \sup_{\tau \in [0, T_f]} |x_1(\tau) - x_2(\tau)|d\tau, \\ &\leq \beta \|x_1 - x_2\| \int_0^{T_f} d\tau, \\ &\leq \beta T_f d(x_1, x_2). \end{aligned}$$

If  $\beta T_f < 1$ , then the Picard mapping  $\psi$  is a contraction. Hence,  $\psi$  has a unique fixed point  $x(t)$  such that

$$(\psi x)(t) = x_0 + \int_0^t G(\tau, x(\tau))d\tau.$$

Using Theorem 1,  $x(t)$  is the solution of (6). □

### Uniqueness

To prove uniqueness of the solution, we let  $x'$  and  $x''$  be two different solutions of (6), then both will be the fixed points of the Picard mapping  $\psi$ , such that

$$(\psi x')(t) = x'(t), \tag{8}$$

$$(\psi x'')(t) = x''(t), \tag{9}$$

where

$$(\psi x')(t) = x'_0 + \int_0^t G(\tau, x'(\tau))d\tau,$$

$$(\psi x'')(t) = x''_0 + \int_0^t G(\tau, x''(\tau))d\tau.$$

Subtracting Equations (8) and (9), and then taking the norm, we obtain

$$\|x'(t) - x''(t)\| = \|x'_0 + \int_0^t G(\tau, x'(\tau))d\tau - x''_0 - \int_0^t G(\tau, x''(\tau))d\tau\|.$$

Since  $(\psi x')(0) = (\psi x'')(0) = (\psi x)(0) = x_0$ ,

$$\begin{aligned} \|x'(t) - x''(t)\| &= \left\| \int_0^t G(\tau, x'(\tau))d\tau - \int_0^t G(\tau, x''(\tau))d\tau \right\|, \\ &\leq \int_0^t \|G(\tau, x'(\tau)) - G(\tau, x''(\tau))\|d\tau, \\ &\leq \beta T_f \|x'(t) - x''(t)\|, \\ (1 - \beta T_f) \|x'(t) - x''(t)\| &\leq 0 \Rightarrow \|x'(t) - x''(t)\| = 0 \Rightarrow x'(t) = x''(t). \end{aligned}$$

Hence, the solution of System (6) is unique.

### 3.2. Boundedness and Positivity

To examine the fundamental properties of Model (5), we show that in a feasible region, the state variables of vector and host populations are bounded and non-negative within a feasible region. First, we show the boundedness of the vector population and the host population, and then prove the positivity of the population.

**Theorem 4.** *The state variables  $\{S, E, I_d, I_m\}$  of the vector population model (2) are bounded within  $\Omega_1 = \{(S, E, I_d, I_m) | 0 \leq N \leq \frac{\Pi}{\nu}\}$ ,  $\forall t \geq 0$ .*

**Proof.** Using Equation (1), we can write

$$\frac{dN}{dt} = \frac{dS}{dt} + \frac{dE}{dt} + \frac{dI_d}{dt} + \frac{dI_m}{dt}. \tag{10}$$

Putting the right-hand side of (2) in Equation (10), the following equation is obtained:

$$\frac{dN}{dt} = \Pi - \nu N, \tag{11}$$

with the condition

$$N(0) \leq \frac{\Pi}{\nu}.$$

Applying the Laplace transformation on (11), we obtain

$$\begin{aligned} \mathcal{L}\left[\frac{dN(t)}{dt}\right] &= \mathcal{L}[\Pi] - \nu \mathcal{L}[\nu N(t)], \\ s(\mathcal{N}(s)) - N(0) &= \frac{\Pi}{s} - \nu \mathcal{N}(s), \\ s(\mathcal{N}(s)) + \nu \mathcal{N}(s) &= \frac{\Pi}{s} + N(0), \\ \mathcal{N}(s) &= \frac{\Pi}{s(s + \nu)} + \frac{N(0)}{s + \nu}. \end{aligned}$$

Using partial fractions, we obtain

$$\mathcal{N}(s) = \frac{\Pi}{\nu} \frac{1}{s} - \frac{\Pi}{\nu} \frac{1}{(s + \nu)} + \frac{N(0)}{s + \nu}. \tag{12}$$

Applying the inverse Laplace transformation on both sides of (12), we obtain

$$\begin{aligned} \mathcal{N}(t) &= \frac{\Pi}{\nu} - \frac{\Pi}{\nu} \exp(-\nu t) + N(0) \exp(-\nu t), \\ &= \frac{\Pi}{\nu} - \left[ \frac{\Pi}{\nu} - N(0) \right] \exp(-\nu t). \end{aligned}$$

Hence, we deduce that

$$\lim_{t \rightarrow \infty} \mathcal{N}(t) \leq \frac{\Pi}{\nu}.$$

□

**Theorem 5.** The state variables =  $\{\mathcal{S}, \mathcal{E}, \mathcal{I}_d, \mathcal{I}_m, \mathcal{I}_{dm}, \mathcal{T}, \mathcal{R}\}$  of the host population Model (4) are also bounded within the feasible region  $\Omega_2 = \{(\mathcal{S}, \mathcal{E}, \mathcal{I}_d, \mathcal{I}_m, \mathcal{I}_{dm}, \mathcal{T}, \mathcal{R}) | 0 \leq \mathcal{N} \leq \frac{\Psi}{\mu}, \forall t \geq 0\}$ .

**Proof.** Taking the derivative of Equation (3) and then substituting the values of the differential equations from (4), we obtain

$$\frac{d\mathcal{N}}{dt} = \Psi - \mu\mathcal{N} - (\delta_{\mathcal{I}_d}\mathcal{I}_d + \delta_{\mathcal{I}_m}\mathcal{I}_m + \delta_{\mathcal{I}_{dm}}\mathcal{I}_{dm} + \delta_{\mathcal{T}}\mathcal{T}). \tag{13}$$

Since  $(\delta_{\mathcal{I}_d}\mathcal{I}_d + \delta_{\mathcal{I}_m}\mathcal{I}_m + \delta_{\mathcal{I}_{dm}}\mathcal{I}_{dm} + \delta_{\mathcal{T}}\mathcal{T}) \geq 0$ , Equation (13) can be written as

$$\frac{d\mathcal{N}}{dt} \leq \Psi - \mu\mathcal{N}, \tag{14}$$

with the condition

$$\mathcal{N}(0) \leq \frac{\Psi}{\mu}.$$

Applying the Laplace transformation to (14) and simplifying gives

$$\mathcal{N}(s) \leq \frac{\Psi}{\mu} \frac{1}{s} - \frac{\Psi}{\mu} \frac{1}{s + \mu} + \frac{\mathcal{N}(0)}{s + \mu}. \tag{15}$$

Applying the inverse Laplace transformation on both sides of (15), we obtain

$$\mathcal{N}(t) \leq \frac{\Psi}{\mu} - \left[ \frac{\Psi}{\mu} - \mathcal{N}(0) \right] \exp(-\mu t).$$

Hence, we can state

$$\lim_{t \rightarrow \infty} \mathcal{N}(t) \leq \frac{\Psi}{\mu}.$$

□

Thus, we proved that the state variables  $(\mathcal{S}, \mathcal{E}, \mathcal{I}_d, \mathcal{I}_m, \mathcal{S}, \mathcal{E}, \mathcal{I}_d, \mathcal{I}_m, \mathcal{I}_{dm}, \mathcal{T}, \mathcal{R})$  of the vectors and human population remains bounded in the feasible region  $\Omega = \max\{\Omega_1, \Omega_2\}$ .

Now, we will show that all state variables of vector and host populations are non-negative for all time  $t > 0$ . For the sake of simplicity, we prove the positivity of one equation and leave the others to be proved in the same way.

**Theorem 6.** Consider Model (5) with non-negative initial conditions (51), the solution  $(\mathcal{S}, \mathcal{E}, \mathcal{I}_d, \mathcal{I}_m, \mathcal{S}, \mathcal{E}, \mathcal{I}_d, \mathcal{I}_m, \mathcal{I}_{dm}, \mathcal{T}, \mathcal{R})$  of Model (5) is non-negative  $\forall t \geq 0$ .

**Proof.** Let us consider the Equation (5a) of the model, i.e.,

$$\frac{d\mathcal{S}}{dt} = \Pi - \frac{(\Phi_1\mathcal{I}_d + \Phi_2\mathcal{I}_m + \Phi_3\mathcal{I}_{dm})\mathcal{S}}{\mathcal{N}} - \nu\mathcal{S}. \tag{16}$$

Since we have proved that all the state variables are bounded, it follows that  $\exists Y \geq 0$  such that:

$$Y = \sup \left[ \frac{\Phi_1\mathcal{I}_d + \Phi_2\mathcal{I}_m + \Phi_3\mathcal{I}_{dm}}{\mathcal{N}} + \nu \right].$$

Thus,

$$\frac{dS}{dt} \geq \Pi - \Upsilon S(t). \tag{17}$$

Applying the Laplace transformation and simplifying, we obtain

$$S(s) \geq \frac{\Pi}{s(s + \Upsilon)} + \frac{S(0)}{s + \Upsilon}.$$

Using partial fractions, we obtain

$$S(s) \geq \frac{\Pi}{\Upsilon} \frac{1}{s} - \frac{\Pi}{\Upsilon} \frac{1}{(s + \Upsilon)} + \frac{S(0)}{s + \Upsilon}. \tag{18}$$

Applying the inverse Laplace transformation on both sides of (18), we obtain

$$S(t) \geq \frac{\Pi}{\Upsilon} - \frac{\Pi}{\Upsilon} \exp(-\Upsilon t) + S(0) \exp(-\Upsilon t). \tag{19}$$

Since  $0 \leq \exp(-\Upsilon t) \leq 1$ ,  $\frac{\Pi}{\Upsilon} \geq \frac{\Pi}{\Upsilon} \exp(-\Upsilon t)$  and also  $S(0) \exp(-\Upsilon t) \geq 0$ .

Thus, it is clear from Equation (19) that  $S(t) > 0, \forall t \geq 0$ . Using a similar approach, we can easily show that all other state variables are also positive  $\forall t \geq 0$ . □

#### 4. Equilibrium Points

Two types of equilibrium points exist for an epidemic model: disease-free equilibrium point and endemic equilibrium point. The disease-free equilibrium (DFE) point of the proposed model is determined to give:

$$P^0 = (S^0, \mathcal{E}^0, \mathcal{I}_d^0, \mathcal{I}_m^0, S^0, E^0, \mathbb{I}_d^0, \mathbb{I}_m^0, \mathbb{I}_{md}^0, T^0, R^0) = \left( \frac{\Pi}{\nu}, 0, 0, 0, \frac{\Psi}{\mu}, 0, 0, 0, 0, 0, 0 \right), \tag{20}$$

and the endemic equilibrium (EE) point of the proposed model is found to give

$$P^1 = (S^1, \mathcal{E}^1, \mathcal{I}_d^1, \mathcal{I}_m^1, S^1, E^1, \mathbb{I}_d^1, \mathbb{I}_m^1, \mathbb{I}_{md}^1, T^1, R^1), \tag{21}$$

where

$$\begin{aligned} \mathcal{E}^1 &= \left[ \frac{\Pi - \nu S^1}{k_1} \right], \mathcal{I}_d^1 = \frac{\Phi_4}{\nu} \left[ \frac{\Pi - \nu S^1}{k_1} \right], \mathcal{I}_m^1 = \frac{\Phi_5}{\nu} \left[ \frac{\Pi - \nu S^1}{k_1} \right], \\ \mathbb{E}^1 &= \left[ \frac{\Psi - \mu S^1}{k_2} \right], \mathbb{I}_d^1 = \frac{\beta_2}{k_3} \left[ \frac{\Psi - \mu S^1}{k_2} \right], \mathbb{I}_m^1 = \frac{\alpha_2}{k_4} \left[ \frac{\Psi - \mu S^1}{k_2} \right], \mathbb{I}_{md}^1 = \frac{\gamma_1}{k_5} \left[ \frac{\Psi - \mu S^1}{k_2} \right], \\ \mathbb{T}^1 &= \left[ \frac{\beta_2 \beta_3}{k_3} + \frac{\alpha_2 \alpha_3}{k_4} + \frac{\gamma_1 \gamma_2}{k_5} \right] \left[ \frac{\Psi - \mu S^1}{k_6 k_2} \right], R^1 = \left[ \frac{\beta_2 \beta_3}{k_3} + \frac{\alpha_2 \alpha_3}{k_4} + \frac{\gamma_1 \gamma_2}{k_5} \right] \left[ \frac{\gamma_3 (\Psi - \mu S^1)}{k_6 k_2 \mu} \right], \end{aligned}$$

with

$$\begin{aligned} k_1 &= \Phi_4 + \Phi_5 + \nu, \quad k_2 = \beta_2 + \alpha_2 + \gamma_1 + \mu, \quad k_3 = \beta_3 + \mu + \delta_{\mathbb{I}_d}, \\ k_4 &= \alpha_3 + \mu + \delta_{\mathbb{I}_m}, \quad k_5 = \gamma_2 + \mu + \delta_{\mathbb{I}_{dm}}, \quad k_6 = \gamma_3 + \mu + \delta_{\mathbb{T}}. \end{aligned}$$

#### Reproduction Number $R_0$

The reproduction number  $R_0$  is a mathematical parameter that ascertains the dispersion of the disease. It signifies the mean or average number of new infections generated by a single infected individual across the entire population. Additionally, it provides the criteria that determine the system’s stability. To develop and determine the reproduction number, a next-generation matrix approach is used. The rate at which a disease spreads through a population is substantially reduced if the basic reproduction number  $R_0$  is less than 1. Under these conditions, the infection will recede and eventually go away. If the

basic reproduction number  $R_0$  is 1, then each infected person will produce exactly a single further case. Therefore, the disease’s prevalence in the population does not fluctuate over the course of its entire duration. The disease spreads more swiftly across the population if the basic reproduction number  $R_0$  is greater than 1. To compute  $R_0$  for the proposed model, we subdivide the classes with infected individuals into  $\mathcal{F}$  and  $\mathcal{V}$ , where

$$\mathcal{F} = \begin{pmatrix} \frac{(\Phi_1\mathbb{I}_d + \Phi_2\mathbb{I}_m + \Phi_3\mathbb{I}_{dm})S}{\mathcal{N}} \\ 0 \\ 0 \\ \frac{(\beta_1\mathcal{I}_d + \alpha_1\mathcal{I}_m)S}{\mathbb{N}} \\ 0 \\ 0 \\ 0 \end{pmatrix},$$

$$\mathcal{V} = \begin{pmatrix} (\Phi_4 + \Phi_5 + \nu)\mathcal{E} \\ -\Phi_4\mathcal{E} + \nu\mathcal{I}_d \\ -\Phi_5\mathcal{E} + \nu\mathcal{I}_m \\ (\beta_2 + \alpha_2 + \gamma_1 + \mu)\mathbb{E} \\ -\beta_2\mathbb{E} + (\beta_3 + \mu + \delta_{\mathbb{I}_d})\mathbb{I}_d \\ -\alpha_2\mathbb{E} + (\alpha_3 + \mu + \delta_{\mathbb{I}_m})\mathbb{I}_m \\ -\gamma_1\mathbb{E} + (\gamma_2 + \mu + \delta_{\mathbb{I}_{dm}})\mathbb{I}_{dm} \end{pmatrix} = \begin{pmatrix} k_1\mathcal{E} \\ -\Phi_4\mathcal{E} + \nu\mathcal{I}_d \\ -\Phi_5\mathcal{E} + \nu\mathcal{I}_m \\ k_2\mathbb{E} \\ -\beta_2\mathbb{E} + k_3\mathbb{I}_d \\ -\alpha_2\mathbb{E} + k_4\mathbb{I}_m \\ -\gamma_1\mathbb{E} + k_5\mathbb{I}_{dm} \end{pmatrix},$$

and then we compute their Jacobian

$$\mathbb{F} = \left( \frac{\partial \mathcal{F}_j}{\partial \mathcal{X}_i} \right)_{p_0}, \quad i, j = 1, 2, 3, 4, 5, 6, 7,$$

$$\mathbb{V} = \left( \frac{\partial \mathcal{V}_j}{\partial \mathcal{X}_i} \right)_{p_0},$$

to give the matrices

$$\mathbb{F} = \begin{pmatrix} 0 & 0 & 0 & 0 & \Phi_1 & \Phi_2 & \Phi_3 \\ 0 & 0 & 0 & 0 & 0 & 0 & 0 \\ 0 & 0 & 0 & 0 & 0 & 0 & 0 \\ 0 & \beta_1 & \alpha_1 & 0 & 0 & 0 & 0 \\ 0 & 0 & 0 & 0 & 0 & 0 & 0 \\ 0 & 0 & 0 & 0 & 0 & 0 & 0 \\ 0 & 0 & 0 & 0 & 0 & 0 & 0 \end{pmatrix},$$

$$\mathbb{V} = \begin{pmatrix} k_1 & 0 & 0 & 0 & 0 & 0 & 0 \\ -\Phi_4 & \nu & 0 & 0 & 0 & 0 & 0 \\ -\Phi_5 & 0 & \nu & 0 & 0 & 0 & 0 \\ 0 & 0 & 0 & k_2 & 0 & 0 & 0 \\ 0 & 0 & 0 & -\beta_2 & k_3 & 0 & 0 \\ 0 & 0 & 0 & -\alpha_2 & 0 & k_4 & 0 \\ 0 & 0 & 0 & -\gamma_1 & 0 & 0 & k_5 \end{pmatrix}.$$

where  $\{\mathcal{X}_1, \mathcal{X}_2, \mathcal{X}_3, \mathcal{X}_4, \mathcal{X}_5, \mathcal{X}_6, \mathcal{X}_7\} = \{\mathcal{E}, \mathcal{I}_d, \mathcal{I}_m, \mathbb{E}, \mathbb{I}_d, \mathbb{I}_m, \mathbb{I}_{dm}\}$ , and at DFE point,  $\mathcal{S}^0 = \mathcal{N}^0 = \frac{\mathbb{N}}{\nu}$  and  $\mathbb{S}^0 = \mathbb{N}^0 = \frac{\Psi}{\mu}$ .

The absolute maximum eigenvalue of the matrix  $\mathbb{F}\mathbb{V}^{-1}$  is computed to give the reproduction number  $R_0$  as:

$$R_0 = \frac{\beta_1\Phi_4 + \alpha_1\Phi_5}{k_1\nu} = \frac{\beta_1\Phi_4 + \alpha_1\Phi_5}{(\Phi_4 + \Phi_5 + \nu)\nu}. \tag{22}$$

The reproduction number ( $R_0$ ) is 3.07 for the values of the parameters given in Table 1. It is clear from Equation (22) that death rate of the mosquitoes are inversely proportional to  $R_0$  and interaction of infectious mosquitoes is directly proportional to the  $R_0$ .

### 5. Stability Analysis

In this section, the local and global stabilities of the dengue–malaria co-infection model (5) are investigated at the DFE and EE points, respectively. When investigating global stabilities, both the Castillo-Chavez approach [42] and the Lyapunov theory with the LaSalle invariance principle [29] are utilized as analytical tools.

#### 5.1. Local Stability at DFE

The Jacobian matrix method is adopted for Model (5) to evaluate its local stability at the DFE point. The Jacobian matrix computed at  $P^0$  is given by

$$J_{P^0} = \begin{pmatrix} -\nu & 0 & 0 & 0 & 0 & 0 & -\Phi_1 & -\Phi_2 & -\Phi_3 & 0 & 0 \\ 0 & -k_1 & 0 & 0 & 0 & 0 & \Phi_1 & \Phi_2 & \Phi_3 & 0 & 0 \\ 0 & \Phi_4 & -\nu & 0 & 0 & 0 & 0 & 0 & 0 & 0 & 0 \\ 0 & \Phi_5 & 0 & -\nu & 0 & 0 & 0 & 0 & 0 & 0 & 0 \\ 0 & 0 & -\beta_1 & -\alpha_1 & -\mu & 0 & 0 & 0 & 0 & 0 & 0 \\ 0 & 0 & \beta_1 & \alpha_1 & 0 & -k_2 & 0 & 0 & 0 & 0 & 0 \\ 0 & 0 & 0 & 0 & 0 & \beta_2 & -k_3 & 0 & 0 & 0 & 0 \\ 0 & 0 & 0 & 0 & 0 & \alpha_2 & 0 & -k_4 & 0 & 0 & 0 \\ 0 & 0 & 0 & 0 & 0 & \gamma_1 & 0 & 0 & -k_5 & 0 & 0 \\ 0 & 0 & 0 & 0 & 0 & 0 & \beta_3 & \alpha_3 & \gamma_2 & -k_6 & 0 \\ 0 & 0 & 0 & 0 & 0 & 0 & 0 & 0 & 0 & \gamma_3 & -\mu \end{pmatrix}. \tag{23}$$

We present the following theorem for local stability of Model (5) at the DFE point  $P^0$ .

**Theorem 7.** Model (5) is locally asymptotically stable (LAS) at  $P^0$  if  $R_0 < 1$  and unstable for  $R_0 > 1$ .

**Proof.** With the assistance of Maple software, we obtain the following eigenvalues of the Jacobian matrix (23).

$$\lambda_1 = -\nu, \tag{24a}$$

$$\lambda_2 = -\nu, \tag{24b}$$

$$\lambda_3 = -\nu, \tag{24c}$$

$$\lambda_4 = -\mu, \tag{24d}$$

$$\lambda_5 = -\mu, \tag{24e}$$

$$\lambda_6 = -k_1, \tag{24f}$$

$$\lambda_7 = -k_2, \tag{24g}$$

$$\lambda_8 = -k_6, \tag{24h}$$

$$\lambda_9 = -\frac{k_3\beta_2\Phi_1}{k_2}(1 - R_0), \tag{24i}$$

$$\lambda_{10} = -k_4\left(1 - \frac{\alpha_2\Phi_2k_3R_0}{\lambda_9k_1k_2\mu}\right), \tag{24j}$$

$$\lambda_{11} = -k_5\left(1 - \frac{k_3k_4\gamma_1R_0}{\lambda_9\lambda_{10}k_1k_2k_5\mu}\right). \tag{24k}$$

It is apparent from Equation (24) that all the eigenvalues are negative when the value of  $R_0$  is less than 1, but not when  $R_0$  is greater than 1. Therefore, it has been demonstrated that

the model represented by System (5) exhibits local asymptotic stability (LAS) when  $R_0 < 1$ , and instability when  $R_0 > 1$ .  $\square$

5.2. Global Stability at DFE

To demonstrate the global stability of the DFE point  $P^0$ , we employ the methodology proposed by Castillo-Chavez [42].

**Theorem 8.** *The DFE point  $P^0$  of Model (5) is GAS if  $R_0 < 1$ , and Conditions (H1) and (H2) are fulfilled:*

$$(H1) \quad \frac{d\mathcal{X}}{dt} = \mathcal{K}(\mathcal{X}, 0) = 0, \quad \mathcal{X}^0 \text{ is GAS,}$$

$$(H2) \quad \frac{d\mathcal{Y}}{dt} = \mathcal{N}(\mathcal{X}, \mathcal{Y}) = \mathcal{B}\mathcal{Y} - \tilde{\mathcal{N}}(\mathcal{X}, \mathcal{Y}),$$

where  $\tilde{\mathcal{N}}(\mathcal{X}, \mathcal{Y}) \geq 0 \quad \forall t \geq 0$  and  $\mathcal{B} = D_{\mathcal{Y}}\mathcal{N}(\mathcal{X}^0, 0)$  is an M-matrix.

**Proof.** Let  $\mathcal{X} = (\mathcal{S}, \mathbb{S})$  represent non-infectious classes and  $\mathcal{Y} = (\mathcal{E}, \mathcal{I}_d, \mathcal{I}_m, \mathbb{E}, \mathbb{I}_d, \mathbb{I}_m, \mathbb{I}_{dm}, \mathbb{T})$  represent infectious classes, and  $P^0 = (\mathcal{X}^0, 0)$  is the DFE point. So,

$$\frac{d\mathcal{X}}{dt} = \mathcal{K}(\mathcal{X}, \mathcal{Y}) = \begin{bmatrix} \Pi - \left( \frac{\Phi_1 \mathbb{I}_d + \Phi_2 \mathbb{I}_m + \Phi_3 \mathbb{I}_{dm}}{\mathcal{N}} + \nu \right) \mathcal{S} \\ \Psi - \left( \frac{\beta_1 \mathcal{I}_d + \alpha_1 \mathcal{I}_m}{\mathbb{N}} + \mu \right) \mathbb{S} \end{bmatrix}. \tag{25}$$

If  $\mathcal{X} = \mathcal{X}^0$ , then  $\mathcal{K}(\mathcal{X}, 0) = 0$ , i.e.,

$$\frac{d\mathcal{X}}{dt} = \begin{bmatrix} \Pi - \nu \mathcal{S}^0 \\ \Psi - \mu \mathbb{S}^0 \end{bmatrix} = \begin{bmatrix} 0 \\ 0 \end{bmatrix}. \tag{26}$$

From Equation (26),  $t \rightarrow \infty, \mathcal{X} \rightarrow \mathcal{X}^0$ . Therefore,  $\mathcal{X}^0$  is GAS. Now,

$$\mathcal{B}\mathcal{Y} - \tilde{\mathcal{N}}(\mathcal{X}, \mathcal{Y}) = \begin{bmatrix} -k_1 & 0 & 0 & 0 & \Phi_1 & \Phi_2 & \Phi_3 & 0 \\ \Phi_4 & -\nu & 0 & 0 & 0 & 0 & 0 & 0 \\ \Phi_5 & 0 & -\nu & 0 & 0 & 0 & 0 & 0 \\ 0 & \beta_1 & \alpha_1 & -k_2 & 0 & 0 & 0 & 0 \\ 0 & 0 & 0 & \beta_2 & -k_3 & 0 & 0 & 0 \\ 0 & 0 & 0 & \alpha_2 & 0 & -k_4 & 0 & 0 \\ 0 & 0 & 0 & \gamma_1 & 0 & 0 & -k_5 & 0 \\ 0 & 0 & 0 & 0 & \beta_3 & \alpha_3 & \gamma_2 & -\gamma_3 \end{bmatrix} \begin{bmatrix} \mathcal{E} \\ \mathcal{I}_d \\ \mathcal{I}_m \\ \mathbb{E} \\ \mathbb{I}_d \\ \mathbb{I}_m \\ \mathbb{I}_{dm} \\ \mathbb{T} \end{bmatrix} - \begin{bmatrix} \kappa_1 \\ 0 \\ 0 \\ \kappa_2 \\ 0 \\ 0 \\ 0 \\ 0 \end{bmatrix}, \tag{27}$$

where

$$\mathcal{B} = \begin{bmatrix} -k_1 & 0 & 0 & 0 & \Phi_1 & \Phi_2 & \Phi_3 & 0 \\ \Phi_4 & -\nu & 0 & 0 & 0 & 0 & 0 & 0 \\ \Phi_5 & 0 & -\nu & 0 & 0 & 0 & 0 & 0 \\ 0 & \beta_1 & \alpha_1 & -k_2 & 0 & 0 & 0 & 0 \\ 0 & 0 & 0 & \beta_2 & -k_3 & 0 & 0 & 0 \\ 0 & 0 & 0 & \alpha_2 & 0 & -k_4 & 0 & 0 \\ 0 & 0 & 0 & \gamma_1 & 0 & 0 & -k_5 & 0 \\ 0 & 0 & 0 & 0 & \beta_3 & \alpha_3 & \gamma_2 & -\gamma_3 \end{bmatrix}, \quad \mathcal{Y} = \begin{bmatrix} \mathcal{E} \\ \mathcal{I}_d \\ \mathcal{I}_m \\ \mathbb{E} \\ \mathbb{I}_d \\ \mathbb{I}_m \\ \mathbb{I}_{dm} \\ \mathbb{T} \end{bmatrix}, \quad \tilde{\mathcal{N}}(\mathcal{X}, \mathcal{Y}) = \begin{bmatrix} \kappa_1 \\ 0 \\ 0 \\ \kappa_2 \\ 0 \\ 0 \\ 0 \\ 0 \end{bmatrix},$$

and  $\kappa_1 = \frac{\Phi_1 \mathbb{I}_d + \Phi_2 \mathbb{I}_m + \Phi_3 \mathbb{I}_{dm}}{\mathcal{N}} (\mathcal{S}_0 - \mathcal{S}), \quad \kappa_2 = \frac{\beta_1 \mathcal{I}_d + \alpha_1 \mathcal{I}_m}{\mathbb{N}} (\mathbb{S}_0 - \mathbb{S}).$

It is evident that  $\mathcal{B}$  is an M-matrix. At the DFE point  $\mathcal{N} = \mathcal{S}^0$  and  $\mathbb{N} = \mathbb{S}^0$ , matrix  $\tilde{\mathcal{N}}(\mathcal{X}, \mathcal{Y}) \geq 0$ . So, the DFE point  $P^0$  is GAS.  $\square$

This means that regardless of the initial circumstances, the model forecasts that the disease will be completely eradicated over time. This consistency shows that public health

initiatives and interventions can successfully slow the disease’s spread, ultimately causing it to go extinct in the community.

5.3. Global Stability at EE

We present the next theorem that shows the global stability of the model (5) EE point  $P^1$ .

**Theorem 9.** *The EE point  $P^1$  of Model (5) is globally stable provided  $R_0 > 1$  and unstable when  $R_0 < 1$ .*

**Proof.** We consider a Volterra-type Lyapunov function defined as

$$\begin{aligned}
 \mathbb{L}(S, \mathcal{E}, \mathcal{I}_d, \mathcal{I}_m, \mathbb{S}, \mathbb{E}, \mathbb{I}_d, \mathbb{I}_m, \mathbb{I}_{dm}, \mathbb{T}, \mathbb{R}) &= \left[ S - S^1 - S^1 \log \frac{S}{S^1} \right] + \left[ \mathcal{E} - \mathcal{E}^1 - \mathcal{E}^1 \log \frac{\mathcal{E}}{\mathcal{E}^1} \right] \\
 &+ \left[ \mathcal{I}_d - \mathcal{I}_d^1 - \mathcal{I}_d^1 \log \frac{\mathcal{I}_d}{\mathcal{I}_d^1} \right] + \left[ \mathcal{I}_m - \mathcal{I}_m^1 - \mathcal{I}_m^1 \log \frac{\mathcal{I}_m}{\mathcal{I}_m^1} \right] \\
 &+ \left[ \mathbb{S} - \mathbb{S}^1 - \mathbb{S}^1 \log \frac{\mathbb{S}}{\mathbb{S}^1} \right] + \left[ \mathbb{E} - \mathbb{E}^1 - \mathbb{E}^1 \log \frac{\mathbb{E}}{\mathbb{E}^1} \right] \\
 &+ \left[ \mathbb{I}_d - \mathbb{I}_d^1 - \mathbb{I}_d^1 \log \frac{\mathbb{I}_d}{\mathbb{I}_d^1} \right] + \left[ \mathbb{I}_m - \mathbb{I}_m^1 - \mathbb{I}_m^1 \log \frac{\mathbb{I}_m}{\mathbb{I}_m^1} \right] \\
 &+ \left[ \mathbb{I}_{dm} - \mathbb{I}_{dm}^1 - \mathbb{I}_{dm}^1 \log \frac{\mathbb{I}_{dm}}{\mathbb{I}_{dm}^1} \right] + \left[ \mathbb{T} - \mathbb{T}^1 - \mathbb{T}^1 \log \frac{\mathbb{T}}{\mathbb{T}^1} \right] \\
 &+ \left[ \mathbb{R} - \mathbb{R}^1 - \mathbb{R}^1 \log \frac{\mathbb{R}}{\mathbb{R}^1} \right],
 \end{aligned} \tag{28}$$

where  $P^1 = (S^1, \mathcal{E}^1, \mathcal{I}_d^1, \mathcal{I}_m^1, \mathbb{S}^1, \mathbb{E}^1, \mathbb{I}_d^1, \mathbb{I}_m^1, \mathbb{I}_{dm}^1, \mathbb{T}^1, \mathbb{R}^1)$  is an EE point.

Taking the derivative of Equation (28) with respect to time  $t$  and then simplifying, we obtain

$$\begin{aligned}
 \frac{d\mathbb{L}}{dt} &= \left[ \frac{S - S^1}{S} \right] \frac{dS}{dt} + \left[ \frac{\mathcal{E} - \mathcal{E}^1}{\mathcal{E}} \right] \frac{d\mathcal{E}}{dt} + \left[ \frac{\mathcal{I}_d - \mathcal{I}_d^1}{\mathcal{I}_d} \right] \frac{d\mathcal{I}_d}{dt} + \left[ \frac{\mathbb{S} - \mathbb{S}^1}{\mathbb{S}} \right] \frac{d\mathbb{S}}{dt} + \left[ \frac{\mathbb{E} - \mathbb{E}^1}{\mathbb{E}} \right] \frac{d\mathbb{E}}{dt} + \\
 &\left[ \frac{\mathbb{I}_d - \mathbb{I}_d^1}{\mathbb{I}_d} \right] \frac{d\mathbb{I}_d}{dt} + \left[ \frac{\mathbb{I}_m - \mathbb{I}_m^1}{\mathbb{I}_m} \right] \frac{d\mathbb{I}_m}{dt} + \left[ \frac{\mathbb{I}_{dm} - \mathbb{I}_{dm}^1}{\mathbb{I}_{dm}} \right] \frac{d\mathbb{I}_{dm}}{dt} + \left[ \frac{\mathbb{T} - \mathbb{T}^1}{\mathbb{T}} \right] \frac{d\mathbb{T}}{dt} + \left[ \frac{\mathbb{R} - \mathbb{R}^1}{\mathbb{R}} \right] \frac{d\mathbb{R}}{dt}.
 \end{aligned}$$

Replacing the time derivatives of state variables with the right-hand sides of the ODEs of Model (5), we reach

$$\frac{d\mathbb{L}}{dt} = \zeta_1 - \zeta_2,$$

where

$$\begin{aligned}
 \zeta_1 &= \left[ \Pi + \left( \frac{\Phi_1 \mathbb{I}_d + \Phi_2 \mathbb{I}_m + \Phi_3 \mathbb{I}_{dm}}{\mathcal{N}} + \nu \right) \frac{(S^1)^2}{S} + \frac{(\Phi_1 \mathbb{I}_d + \Phi_2 \mathbb{I}_m + \Phi_3 \mathbb{I}_{dm}) S}{\mathcal{N}} + (\Phi_4 + \Phi_5 + \nu) \frac{(\mathcal{E}^1)^2}{\mathcal{E}} \right. \\
 &+ \Phi_4 \mathcal{E} + (\nu) \frac{(\mathcal{I}_d^1)^2}{\mathcal{I}_d} + \Phi_5 \mathcal{E} + (\nu) \frac{(\mathcal{I}_m^1)^2}{\mathcal{I}_m} + \Psi + \left( \frac{\beta_1 \mathcal{I}_d + \alpha_1 \mathcal{I}_m}{\mathcal{N}} + \mu \right) \frac{(S^1)^2}{S} + \frac{(\beta_1 \mathcal{I}_d + \alpha_1 \mathcal{I}_m) S}{\mathcal{N}} \\
 &+ \beta_2 \mathbb{E} + (\beta_2 + \alpha_2 + \gamma_1 + \mu) \frac{(\mathbb{E}^1)^2}{\mathbb{E}} + (\beta_3 + \mu + \delta_{\mathbb{I}_d}) \frac{(\mathbb{I}_d^1)^2}{\mathbb{I}_d} + \alpha_2 \mathbb{E} + (\alpha_3 + \mu + \delta_{\mathbb{I}_m}) \frac{(\mathbb{I}_m^1)^2}{\mathbb{I}_m} \\
 &+ \gamma_1 \mathbb{E} + (\gamma_2 + \mu + \delta_{\mathbb{I}_{dm}}) \frac{(\mathbb{I}_{dm}^1)^2}{\mathbb{I}_{dm}} + \beta_3 \mathbb{I}_d + \alpha_3 \mathbb{I}_m + \gamma_2 \mathbb{I}_{dm} + (\gamma_3 + \mu + \delta_{\mathbb{T}}) \frac{(\mathbb{T}^1)^2}{\mathbb{T}} + \gamma_3 \mathbb{T} \\
 &\left. + \mu \frac{(\mathbb{R}^1)^2}{\mathbb{R}} \right],
 \end{aligned}$$

and

$$\begin{aligned} \zeta_2 = & \left[ \left( \frac{\Phi_1 \mathbb{I}_d + \Phi_2 \mathbb{I}_m + \Phi_3 \mathbb{I}_{dm}}{\mathcal{N}} + \nu \right) \frac{(\mathcal{S} - \mathcal{S}^1)^2}{\mathcal{S}} + \Pi \frac{\mathcal{S}^1}{\mathcal{S}} + \left( \frac{\Phi_1 \mathbb{I}_d + \Phi_2 \mathbb{I}_m + \Phi_3 \mathbb{I}_{dm}}{\mathcal{N}} + \nu \right) \mathcal{S}^1 \right. \\ & + \frac{\mathcal{I}_d^1}{\mathcal{I}_d} \Phi_4 \mathcal{E} + \frac{(\mathcal{E} - \mathcal{E}^1)^2}{\mathcal{E}} (\Phi_4 + \Phi_5 + \nu) + \frac{\mathcal{E}^1}{\mathcal{E}} \left( \frac{\Phi_1 \mathbb{I}_d + \Phi_2 \mathbb{I}_m + \Phi_3 \mathbb{I}_{dm}}{\mathcal{N}} \right) \mathcal{S} + (\Phi_4 + \Phi_5 + \nu) \mathcal{E}^1 \\ & + \frac{(\mathcal{I}_d - \mathcal{I}_d^1)^2}{\mathcal{I}_d} \nu + \frac{(\mathcal{I}_m - \mathcal{I}_m^1)^2}{\mathcal{I}_m} \nu + \frac{\mathcal{I}_m^1}{\mathcal{I}_m} \Phi_5 \mathcal{E} + \nu \mathcal{I}_m^1 + \left( \frac{\beta_1 \mathcal{I}_d + \alpha_1 \mathcal{I}_m}{\mathbb{N}} + \mu \right) \frac{(\mathcal{S} - \mathcal{S}^1)^2}{\mathcal{S}} \\ & + \Psi \frac{\mathcal{S}^1}{\mathbb{S}} + \left( \frac{\beta_1 \mathbb{I}_d + \alpha_1 \mathbb{I}_m}{\mathbb{N}} + \mu \right) \mathbb{S}^1 + \frac{(\mathbb{E} - \mathbb{E}^1)^2}{\mathbb{E}} (\beta_2 + \alpha_2 + \gamma_1 + \mu) + \frac{\mathbb{E}^1}{\mathbb{E}} \left( \frac{\beta_1 \mathcal{I}_d + \alpha_1 \mathcal{I}_m}{\mathbb{N}} \right) \mathbb{S} \\ & + (\beta_2 + \alpha_2 + \gamma_1 + \mu) \mathbb{E}^1 + \frac{(\mathbb{I}_d - \mathbb{I}_d^1)^2}{\mathbb{I}_d} (\beta_3 + \mu + \delta_{\mathbb{I}_d}) + \nu \mathcal{I}_d^1 + \frac{\mathbb{I}_d^1}{\mathbb{I}_d} \beta_2 \mathbb{E} + (\beta_3 + \mu + \delta_{\mathbb{I}_d}) \mathbb{I}_d^1 \\ & + \frac{(\mathbb{I}_m - \mathbb{I}_m^1)^2}{\mathbb{I}_m} (\alpha_3 + \mu + \delta_{\mathbb{I}_m}) + \frac{\mathbb{I}_m^1}{\mathbb{I}_m} \alpha_2 \mathbb{E} + (\alpha_3 + \mu + \delta_{\mathbb{I}_m}) \mathbb{I}_m^1 + \frac{(\mathbb{I}_{dm} - \mathbb{I}_{dm}^1)^2}{\mathbb{I}_{dm}} (\gamma_2 + \mu + \delta_{\mathbb{I}_{dm}}) \\ & + \frac{\mathbb{I}_{dm}^1}{\mathbb{I}_{dm}} \gamma_1 \mathbb{E} + (\gamma_2 + \mu + \delta_{\mathbb{I}_{dm}}) \mathbb{I}_{dm}^1 + \frac{(\mathbb{T} - \mathbb{T}^1)^2}{\mathbb{T}} (\gamma_3 + \mu + \delta_{\mathbb{T}}) + \frac{\mathbb{T}^1}{\mathbb{T}} (\beta_3 \mathbb{I}_d + \alpha_3 \mathbb{I}_m + \gamma_2 \mathbb{I}_{dm}) \\ & \left. + (\gamma_3 + \mu + \delta_{\mathbb{T}}) \mathbb{T}^1 + \mu \frac{(\mathbb{R} - \mathbb{R}^1)^2}{\mathbb{R}} + \mu \mathbb{R}^1 + \frac{\mathbb{R}^1}{\mathbb{R}} (\gamma_3 \mathbb{T}) \right]. \end{aligned}$$

As we know for  $R_0 < 1$ ,  $\mathcal{N} = \mathcal{S}$ ,  $\mathcal{E} = \mathcal{I}_d = \mathcal{I}_m = 0$  and  $\mathbb{N} = \mathbb{S}$ ,  $\mathbb{E} = \mathbb{I}_d = \mathbb{I}_m = \mathbb{I}_{dm} = \mathbb{T} = \mathbb{R} = 0$ . Therefore, for  $R_0 > 1$ , all the state variables are increasing functions except  $\mathcal{S}$  and  $\mathbb{S}$  (that are decreasing) and bounded by endemic equilibrium point  $P^1$ . Now it is clear that  $\zeta_2 > \zeta_1$  and  $\frac{d\mathcal{L}}{dt} < 0$  except at EE point.

Now, if we put EE point,  $\mathcal{S} = \mathcal{S}^1$ ,  $\mathcal{E} = \mathcal{E}^1$ ,  $\mathcal{I}_d = \mathcal{I}_d^1$ ,  $\mathcal{I}_m = \mathcal{I}_m^1$ ,  $\mathbb{S} = \mathbb{S}^1$ ,  $\mathbb{E} = \mathbb{E}^1$ ,  $\mathbb{I}_d = \mathbb{I}_d^1$ ,  $\mathbb{I}_m = \mathbb{I}_m^1$ ,  $\mathbb{I}_{dm} = \mathbb{I}_{dm}^1$ ,  $\mathbb{T} = \mathbb{T}^1$ , and  $\mathbb{R} = \mathbb{R}^1$ , then

$$\begin{aligned} \zeta_1 = & \left[ \Pi + \left( \frac{\Phi_1 \mathbb{I}_d^1 + \Phi_2 \mathbb{I}_m^1 + \Phi_3 \mathbb{I}_{dm}^1}{\mathcal{N}^1} + \nu \right) (\mathcal{S}^1) + \frac{(\Phi_1 \mathbb{I}_d^1 + \Phi_2 \mathbb{I}_m^1 + \Phi_3 \mathbb{I}_{dm}^1) \mathcal{S}^1}{\mathcal{N}^1} + \Phi_4 \mathcal{E}^1 \right. \\ & + (\Phi_4 + \Phi_5 + \nu) (\mathcal{E}^1) + (\nu) (\mathcal{I}_d^1) + \Phi_5 \mathcal{E}^1 + (\nu) (\mathcal{I}_m^1) + \Psi + \left( \frac{\beta_1 \mathcal{I}_d^1 + \alpha_1 \mathcal{I}_m^1}{\mathbb{N}^1} + \mu \right) (\mathbb{S}^1) \\ & + \frac{(\beta_1 \mathcal{I}_d^1 + \alpha_1 \mathcal{I}_m^1) \mathbb{S}^1}{\mathbb{N}^1} + \beta_2 \mathbb{E}^1 + (\beta_2 + \alpha_2 + \gamma_1 + \mu) (\mathbb{E}^1) + (\beta_3 + \mu + \delta_{\mathbb{I}_d}) (\mathbb{I}_d^1) + \alpha_2 \mathbb{E}^1 \\ & + (\alpha_3 + \mu + \delta_{\mathbb{I}_m}) (\mathbb{I}_m^1) + \gamma_1 \mathbb{E}^1 + (\gamma_2 + \mu + \delta_{\mathbb{I}_{dm}}) (\mathbb{I}_{dm}^1) + \beta_3 \mathbb{I}_d^1 + \alpha_3 \mathbb{I}_m^1 + \gamma_2 \mathbb{I}_{dm}^1 \\ & \left. + (\gamma_3 + \mu + \delta_{\mathbb{T}}) (\mathbb{T}^1) + \gamma_3 \mathbb{T}^1 + \mu (\mathbb{R}^1) \right], \end{aligned}$$

and

$$\begin{aligned} \zeta_2 = & \left[ \Pi + \left( \frac{\Phi_1 \mathbb{I}_d^1 + \Phi_2 \mathbb{I}_m^1 + \Phi_3 \mathbb{I}_{dm}^1}{\mathcal{N}^1} + \nu \right) \mathcal{S}^1 + \Phi_4 \mathcal{E}^1 + \left( \frac{\Phi_1 \mathbb{I}_d^1 + \Phi_2 \mathbb{I}_m^1 + \Phi_3 \mathbb{I}_{dm}^1}{\mathcal{N}^1} \right) \mathcal{S}^1 \right. \\ & + (\Phi_4 + \Phi_5 + \nu) \mathcal{E}^1 + \Phi_5 \mathcal{E}^1 + \nu \mathcal{I}_m^1 + \Psi + \left( \frac{\beta_1 \mathcal{I}_d^1 + \alpha_1 \mathcal{I}_m^1}{\mathbb{N}^1} + \mu \right) \mathbb{S}^1 + \left( \frac{\beta_1 \mathcal{I}_d^1 + \alpha_1 \mathcal{I}_m^1}{\mathbb{N}^1} \right) \mathbb{S}^1 \\ & + (\beta_2 + \alpha_2 + \gamma_1 + \mu) \mathbb{E}^1 + \nu \mathcal{I}_d^1 + \beta_2 \mathbb{E}^1 + (\beta_3 + \mu + \delta_{\mathbb{I}_d}) \mathbb{I}_d^1 + \alpha_2 \mathbb{E}^1 + (\alpha_3 + \mu + \delta_{\mathbb{I}_m}) \mathbb{I}_m^1 \\ & \left. + \gamma_1 \mathbb{E}^1 + (\gamma_2 + \mu + \delta_{\mathbb{I}_{dm}}) \mathbb{I}_{dm}^1 + \beta_3 \mathbb{I}_d^1 + \alpha_3 \mathbb{I}_m^1 + \gamma_2 \mathbb{I}_{dm}^1 + (\gamma_3 + \mu + \delta_{\mathbb{T}}) \mathbb{T}^1 + \mu \mathbb{R}^1 + (\gamma_3 \mathbb{T}^1) \right]. \end{aligned}$$

Thus,  $\frac{d\mathcal{L}}{dt} = 0$  at EE point  $P^1$ .

$$\frac{d\mathcal{L}}{dt} \leq 0.$$

Thus, according to LaSalle’s invariance principle [43], the EE point  $P^1$  is globally asymptotically stable.  $\square$

### 6. Sensitivity Analysis

Developing effective methods for controlling the spread of viruses requires critical sensitivity analysis. This analytical process involves identifying parameters that are highly sensitive to  $R_0$ , the basic reproduction number. Parameters with a high sensitivity index are considered highly sensitive to  $R_0$  and can be targeted for epidemic control efforts. In this study, we utilized the approach, outlined in [44], to calculate the sensitivity index of a parameter  $p$  using the following formula:

$$\eta_p^{R_0} = \frac{\partial R_0}{\partial p} \frac{p}{R_0}.$$

We compute sensitivity indices of all parameters that are involved in  $R_0$  and present the results in Table 2. The sensitivity analysis gives the information that  $\alpha_1$ , the interaction rate of malaria, and  $\Phi_5$ , the transmission rate of malaria infection are the most sensitive parameters to  $R_0$ . Overall, sensitivity analysis is a valuable tool for identifying the parameters that are most important in controlling the spread of viruses.

**Table 2.** Sensitivity index for  $R_0$ .

Parameter	Sensitivity Index	Relationship
$\nu$	−1.049353483	Inverse
$\beta_1$	0.005622975459	Direct
$\alpha_1$	2.451326865	Direct
$\Phi_4$	−0.6706816119	Inverse
$\Phi_5$	0.7200350942	Direct

Table 2 presents the results indicating that the variables  $\beta_1$ ,  $\alpha_1$ , and  $\phi_5$  have a positive impact on the  $R_0$ , while the variables  $\nu$  and  $\phi_4$  have a negative impact on the  $R_0$ . This implies that a variation of 10% in these factors would lead to a proportional 10% change in the  $R_0$ . For instance, an increase of 10% in the values of  $\beta_1$ ,  $\alpha_1$ , and  $\phi_5$  results in a corresponding increase of 0.0562%, 24.5132%, and 7.2003% in  $R_0$ , respectively. In a similar manner, an increase of 10% in the values of  $\nu$  and  $\phi_4$  results in a decrease of 10.4935% and 6.7068% respectively in the value of Tables 3 and 4 represent the qualitative (numeric) version of the Figure 2 and validate the graphical results. Our sensitivity analysis indicates that the death rate of mosquitoes and the interaction rate of the infectious mosquitoes have a direct impact on the dengue–malaria co-infection spreads and are the most suitable parameters to serve as control variables to control the spread of the disease. Therefore, we use these rates (parameters) as control parameters and show the importance of these control strategies in the next section with details. To understand the influence of the two parameters on  $R_0$ , we vary  $\Phi_5$  and  $\nu$  (Figure 3). Similarly, we investigate the effect on  $R_0$  when varying  $\beta_1$  and  $\Phi_4$  (Figure 4) and varying  $\alpha_1$  and  $\nu$  (Figure 5).

**Table 3.**  $\nu$  vs.  $R_0$ .

$\nu$	$R_0$
0.100	1.5415
0.200	0.7071
0.300	0.4354
0.400	0.3034

**Table 3.** Cont.

$\nu$	$R_0$
0.500	0.2266
0.600	0.1771
0.700	0.1429
0.800	0.1181
0.900	0.0995
1.000	0.0851

**Table 4.**  $\beta_1$  vs.  $R_0$ .

$\beta_1$	$R_0$
0.000	3.0540
0.100	4.3437
0.200	5.6334
0.300	6.9230
0.400	8.2127
0.500	9.5024
0.600	10.7920
0.700	12.0817
0.800	13.3714
0.900	14.6611
1.000	15.9507

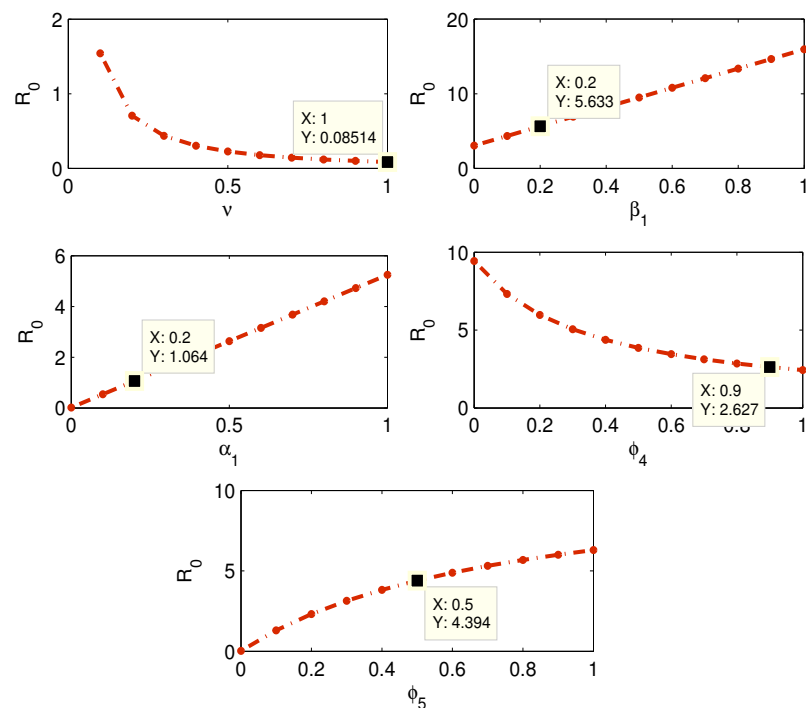


**Figure 2.** Effect of each parameter on  $R_0$ .

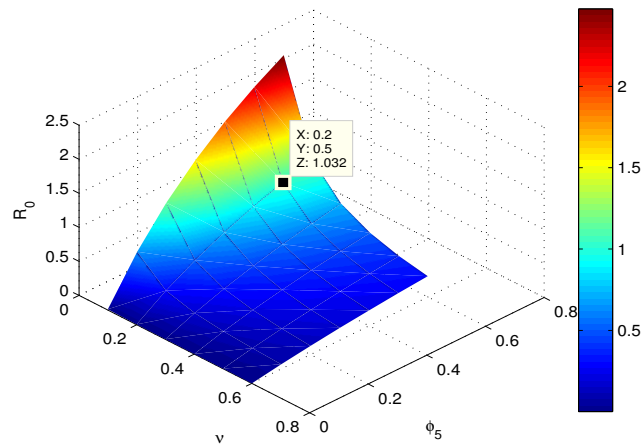


Figure 3. Navigating the epidemic landscape with the interplay of  $\Phi_5$  and  $\nu$  on  $R_0$  with colormap.

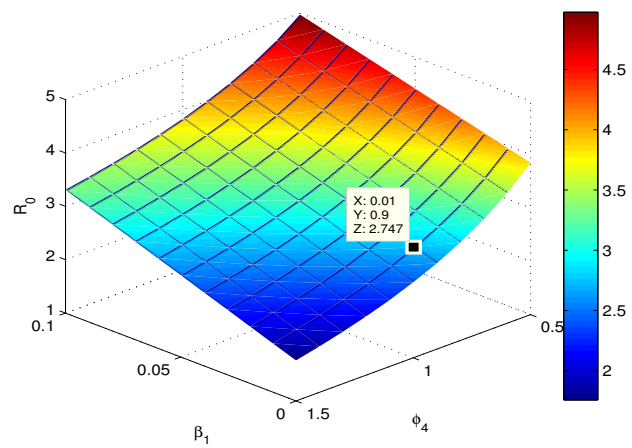


Figure 4. Epidemic insights in 3D by visualizing  $R_0$  sensitivity to  $\beta_1$  and  $\Phi_4$ .

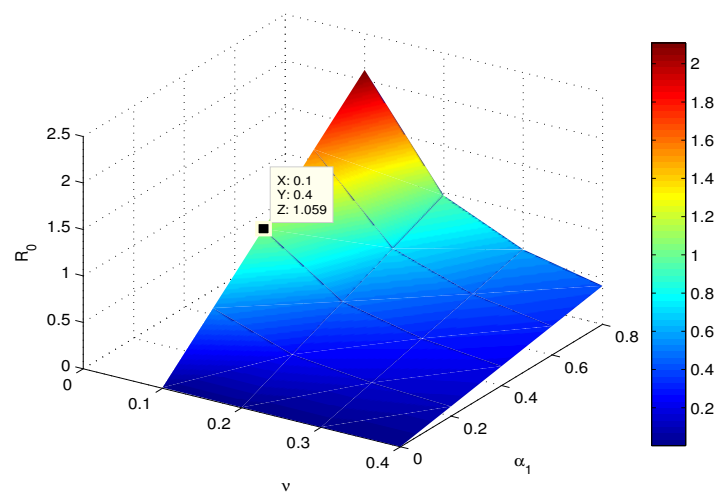


Figure 5. Navigating epidemic dynamics by visualizing  $R_0$  sensitivity to  $\alpha_1$  and  $\nu$  with a colormap.

### 7. Effects of the Control Strategies

In order to manage the dengue–malaria disease, we incorporate three new control parameters into Model (5), named as  $u_1$ ,  $u_2$ , and  $u_3$ . Specifically,  $u_1$  represents the use of spray,  $u_2$  represents self-precaution, and  $u_3$  represents the reduction of human–mosquito interaction. We evaluate the impact of each of these parameters separately. The model updates are illustrated as a flow diagram, see Figure 6, and as model equations for co-infection given as:

$$\frac{dS}{dt} = \Pi - \frac{(\Phi_1 I_d + \Phi_2 I_m + \Phi_3 I_{dm})S}{N} - (\nu + u_1)S, \tag{29a}$$

$$\frac{dE}{dt} = \frac{(\Phi_1 I_d + \Phi_2 I_m + \Phi_3 I_{dm})S}{N} - (\Phi_4 + \Phi_5 + \nu + u_1)E, \tag{29b}$$

$$\frac{dI_d}{dt} = \Phi_4 E - (\nu + u_1)I_d, \tag{29c}$$

$$\frac{dI_m}{dt} = \Phi_5 E - (\nu + u_1)I_m, \tag{29d}$$

$$\frac{dS}{dt} = \Psi - (1 - u_3) \frac{(\beta_1 I_d + \alpha_1 I_m)S}{N} - (\mu + u_2)S, \tag{29e}$$

$$\frac{dE}{dt} = (1 - u_3) \frac{(\beta_1 I_d + \alpha_1 I_m)S}{N} - (\beta_2 + \alpha_2 + \gamma_1 + \mu)E, \tag{29f}$$

$$\frac{dI_d}{dt} = \beta_2 E - (\beta_3 + \mu + \delta_{I_d})I_d, \tag{29g}$$

$$\frac{dI_m}{dt} = \alpha_2 E - (\alpha_3 + \mu + \delta_{I_m})I_m, \tag{29h}$$

$$\frac{dI_{dm}}{dt} = \gamma_1 E - (\gamma_2 + \mu + \delta_{I_{dm}})I_{dm}, \tag{29i}$$

$$\frac{dT}{dt} = \beta_3 I_d + \alpha_3 I_m + \gamma_2 I_{dm} - (\gamma_3 + \mu + \delta_T)T, \tag{29j}$$

$$\frac{dR}{dt} = \gamma_3 T - \mu R + u_2 S, \tag{29k}$$

with non-negative initial conditions:

$$\begin{aligned} S(0) = S_0 > 0, \quad E(0) = E_0 \geq 0, \quad I_d(0) = I_{d0} \geq 0, \quad I_m(0) = I_{m0} \geq 0, \quad S(0) = S_0 > 0, \\ E(0) = E_0 \geq 0, \quad I_d(0) = I_{d0} \geq 0, \quad I_m(0) = I_{m0} \geq 0, \quad I_{dm}(0) = I_{dm0} \geq 0, \quad T(0) = T_0 \geq 0, \\ R(0) = R_0. \end{aligned} \tag{29l}$$

#### 7.1. Numerical Discretization and Results

We divide the continuous domain  $[0, T_f]$  into  $N + 1$  evenly spaced discrete points  $t_j = jh, j = 0, 1, 2, \dots, N$ , where  $h = \frac{T_f}{N}$ ,  $T_f$  represents the final time and  $N$  is the number of intervals. To solve the system of differential equations described in (29) on this discretized domain, we utilize the widely recognized and dependable numerical method known as the fourth-order Runge–Kutta method (RK-4). The subsequent section of this work includes three distinct cases, each featuring a different spray and non-pharmaceutical control strategy. Further elaboration and discussion on each case can be found below.

#### 7.2. Effect of Spray (Case 1)

For Case 1, we consider  $u_1 \neq 0$  and take  $u_2 = u_3 = 0$ , in our proposed model (i.e., we only intend to study the impact of mosquito killing spray on disease control). Our findings indicate that this control strategy had a significant impact in managing the dengue–malaria co-infection disease (Figures 7 and 8). As a vector-borne disease, reducing the population of disease-carrying mosquitoes directly translates to a decrease in the interactions between healthy humans and infected mosquitoes and vice versa. Our analysis of the effectiveness of the spray control strategy strongly supports this assertion, as we observe a shift in

the system dynamics from an endemic state to a disease-free state. Overall, our results suggest that the use of spray is a valuable control measure for managing dengue–malaria co-infection.

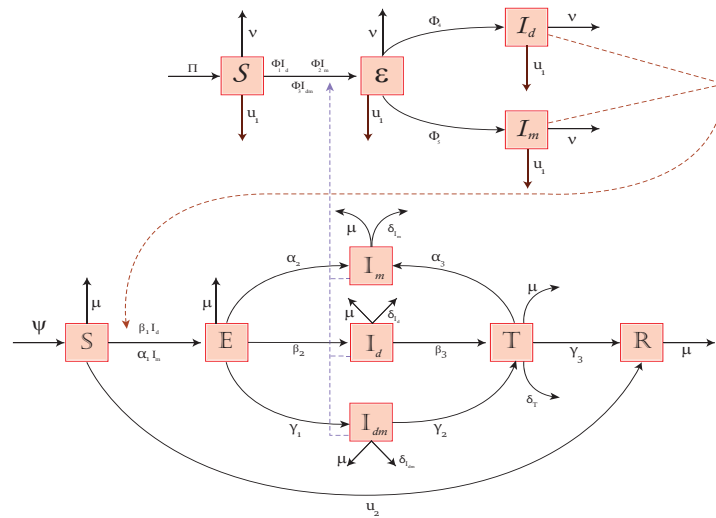


**Figure 6.** Updated co-infection flow diagram: Similar to Figure 1 but with three additional control parameters, named as spray for mosquitoes ( $u_1$ ), self-precautions ( $u_2$ ), and intervention to reduce the humans-mosquitoes interactions ( $u_3$ ).

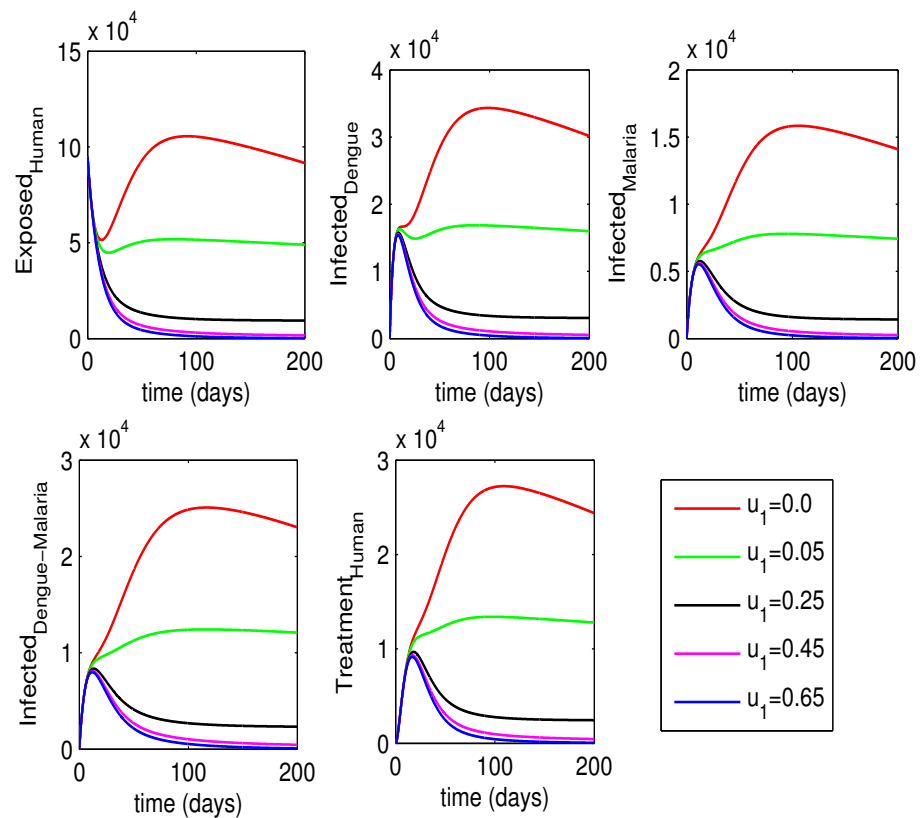


**Figure 7.** Effect of spray rate  $u_1$  on the infectious human state variables. The dynamics indicate that we can control the spread of disease by eradicating the mosquitoes using spray.

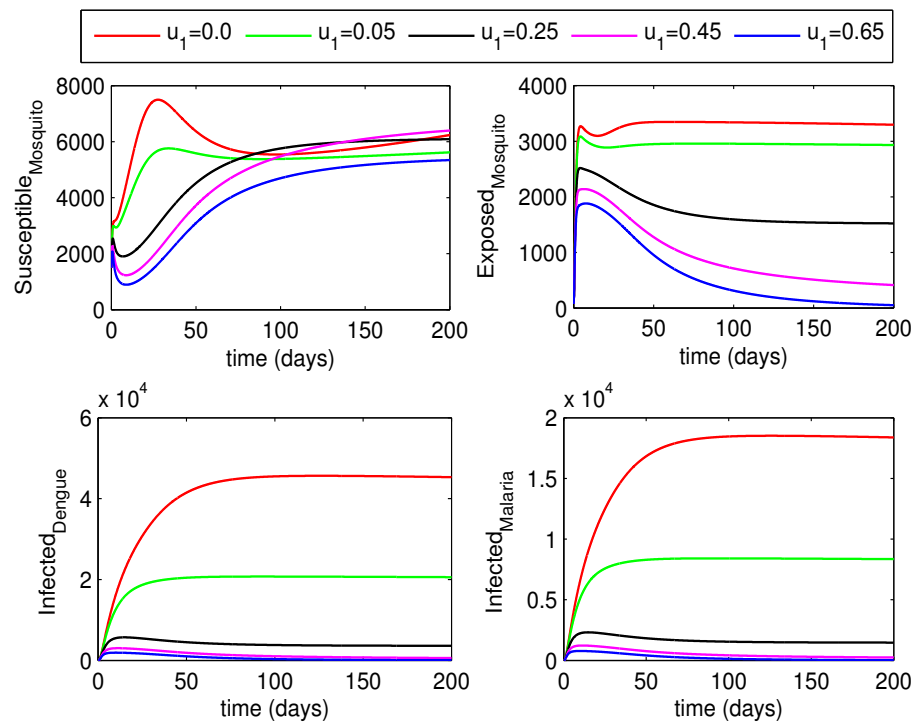


Figure 8. Effect of spray rate  $u_1$  on the mosquitoes state variables.

7.3. Self-Protection (Case 2)

In Case 2, susceptible humans adopt a control parameter for self-protection denoted by  $u_2$ , which varies in value, while  $u_1$  and  $u_3$  remain constantly zero. The control parameter  $u_2$  represents self-precaution measures, such as using bed nets, mosquito repellent lotion, and full sleeves. There is a significant effect of control parameter  $u_2$  on human and vector populations (Figures 9 and 10) and on controlling the spread of dengue–malaria co-infection. Our mathematical analysis indicates that the disease will die out from the community if 35% of the susceptible follow the precautions. The results also indicate that the dynamical system shifts rapidly from the endemic position to the disease-free position when self-precaution is practiced. Thus, self-precaution is an easy and effective measure for controlling dengue–malaria co-infection.

7.4. Reduction in the Infectious Interactions (Case 3)

For Case 3, we consider various levels of  $u_3$ , which correspond to different degrees of reduction in interaction rates. In this scenario, the controls  $u_1$  and  $u_2$  are set to zero. We conducted an analysis by gradually decreasing the interaction level from 100% to 35% by increasing  $u_3$  from 0% to 65% and found that the system did not transition to an endemic state as in the previous two cases (Figures 11 and 12). However, reducing interactions is often difficult in practice as it incurs significant financial costs. By decreasing the interaction between infectious vector populations and susceptible humans, we indirectly reduce the recruitment rate of the infection and directly impact the rate of interaction with infectious humans. This is because the reduction in infectious humans leads to a decrease in the rate of interaction. Our analysis illustrates that all strategies reduce the disease burden (Figures 7–12), but the most effective and feasible one is to take self-precautionary measures, such as cleaning and drying stored water, and wearing appropriate clothing. According to our mathematical analysis, the second most effective strategy is to spray or eliminate infected vectors from houses and other potential resistance points.

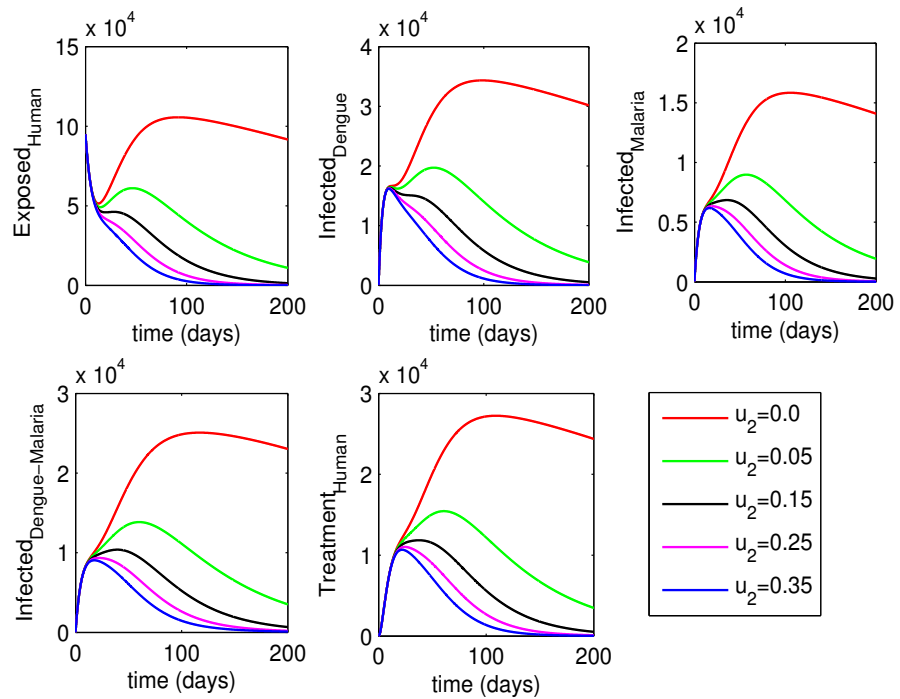


**Figure 9.** Effect of self-precaution rate  $u_2$  on the infectious human state variables. If more people adopt the self-precaution, then chance of interaction of human and mosquitoes decreases and disease will die.

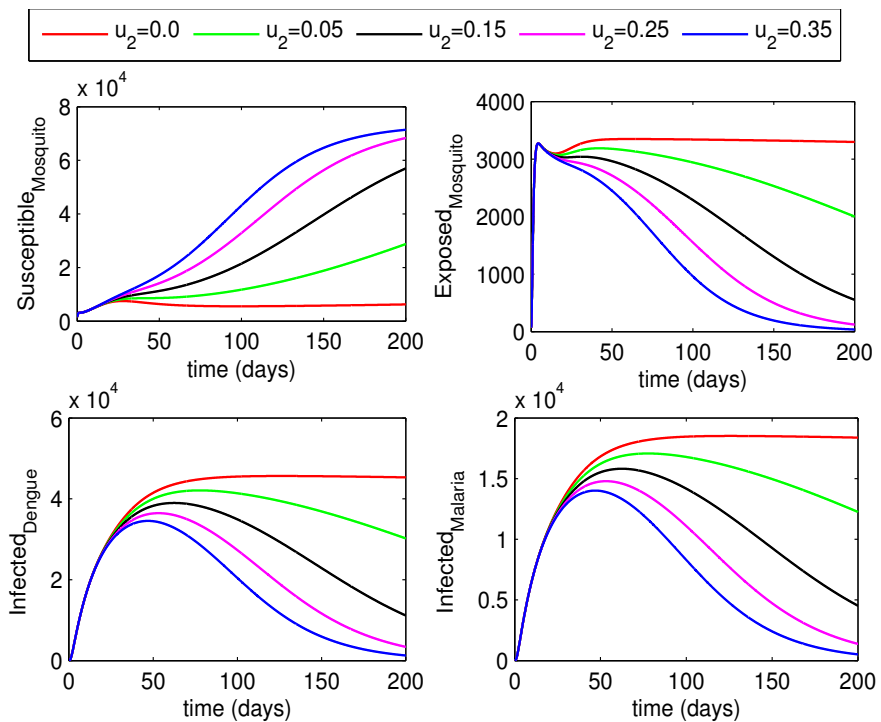


**Figure 10.** Effect of self-precaution rate  $u_2$  on the mosquitoes' state variables.

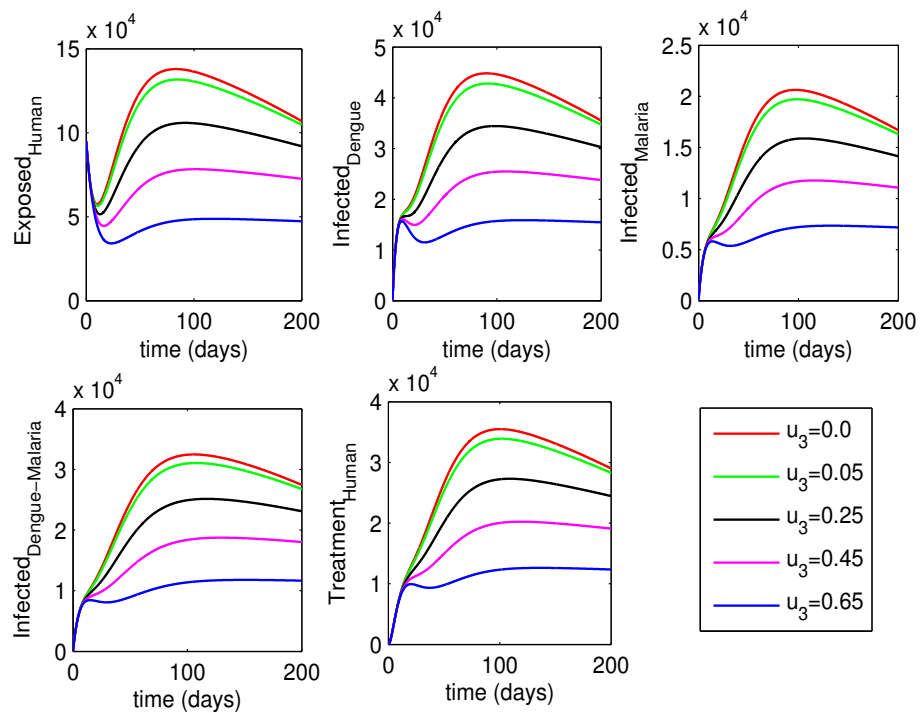


Figure 11. Effect of the interaction rate ( $u_3$ ) of infectious mosquitoes and humans on the infectious human state variables.

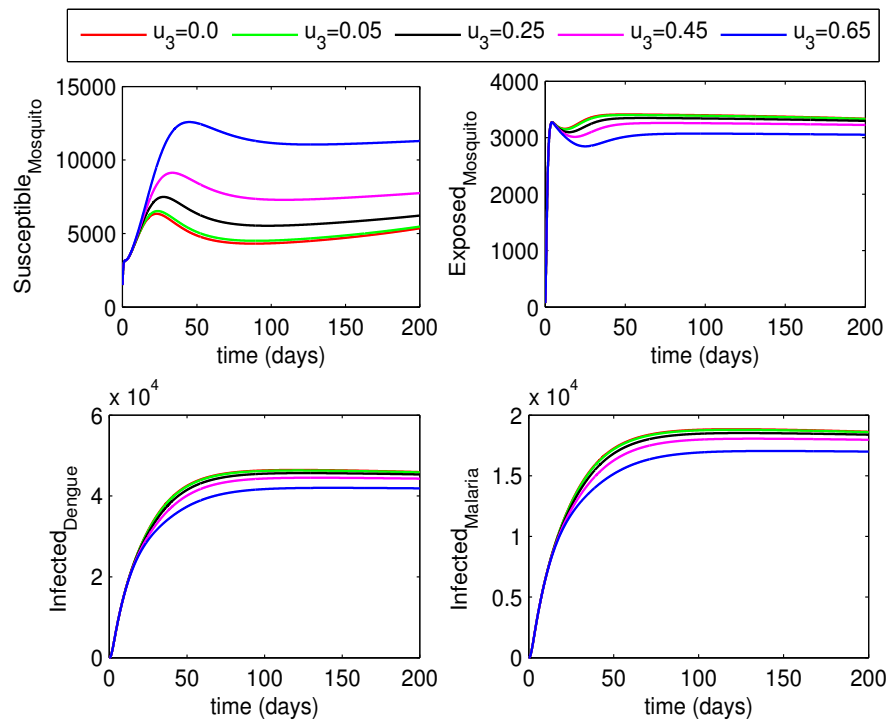


Figure 12. Effect of the interaction rate ( $u_3$ ) of infectious mosquitoes and humans on the mosquitoes' state variables.

### 8. Conclusions

We proposed a new mathematical model for dengue–malaria co-infection to observe the disease-spreading pattern and control analysis. We proved the physical and biological properties associated with the model, (i.e., the existence of unique positive and bounded solutions in a physical region). To understand the dynamics of the disease, both equilibrium points (disease-free and endemic) were also calculated. At equilibrium points, we

demonstrated that the model is both locally and globally stable. We also performed a sensitivity analysis to see how the parameters of the model affect the reproduction number  $R_0$  and identified the most influential parameters.

We updated our proposed mathematical model with three additional control parameters, representing spray for mosquitoes, self-precaution, and reduction in mosquito–human interaction rates. We analyzed the effect of each varying control parameter. Control analysis for the proposed model tells us that all the control parameters are beneficial to control disease, but the most reasonable and easy to adopt is self-precaution or self-protection. Humans can protect themselves easily by taking basic precautions. The second most effective parameter is spray on the vector’s population. It is also obvious that disease will die out if the vector population decreases.

Our research highlights a significant advancement in the field of disease prevention by adding three new control parameters representing mosquito spraying, self-precaution, and reduction of mosquito–human contact to the proposed mathematical model. A careful examination of these factors revealed their significant influence on the treatment of illness. The main conclusions show that all control parameters are successful in preventing the spread of disease; however, self-precaution stands out as the most workable and accessible tactic, highlighting the significance of taking simple precautions for personal safety. Moreover, spraying is the second most successful method for managing the mosquito vector population. Notably, the study shows that the disease may be eliminated as long as the vector population is steadily decreasing, highlighting the importance of these results in developing more approachable and effective disease management methods.

In order to see how fractional order affects the dynamics of dengue–malaria co-infection, a future study is going to involve a clear picture of the disease dispersion using a fractional model with an ABC derivative operator and various intervention options. The ABC operator was selected because its kernel is non-local and non-singular. When compared to other fractional operators (Caputo, Caputo-Fabrizio), the ABC operator is able to capture more susceptibilities while simultaneously reducing infections. We will also analyze a fractional-order optimal control problem to find the best strategies for vaccination and hospitalization.

**Author Contributions:** Conceptualization, A.I.K.B. and M.I.; methodology, A.I.K.B. and M.I.; software, A.I.K.B. and M.I.; validation, B.A.M., H.A., and S.B.; formal analysis, A.I.K.B. and M.I.; investigation, B.A.M. and A.I.K.B.; resources, B.A.M. and S.B.; data curation, S.B. and H.A.; writing—original draft preparation, M.I.; writing—review and editing, A.I.K.B. and B.A.M.; visualization, M.I. and S.B.; supervision, A.I.K.B. and B.A.M.; project administration, A.I.K.B. and M.I.; funding acquisition, A.I.K.B. All authors have read and agreed to the published version of the manuscript.

**Funding:** This work was supported by the Deanship of Scientific Research, Vice Presidency for Graduate Studies and Scientific Research, King Faisal University, Saudi Arabia (Project No. GRANT4972).

**Data Availability Statement:** All data supporting the findings of this study are available within the paper.

**Acknowledgments:** The authors would like to acknowledge the support from King Faisal University, Saudi Arabia, and Tandy School of Computer Science, University of Tulsa, USA.

**Conflicts of Interest:** The authors declare no conflict of interest.

## References

1. Modahl, C.M.; Chowdhury, A.; Low, D.H.W.; Manuel, M.C.; Missé, D.; Kini, R.M.; Mendenhall, I.H.; Pompon, J. Midgut transcriptomic responses to dengue and chikungunya viruses in the vectors *Aedes albopictus* and *Aedes malayensis*. *Sci. Rep.* **2023**, *13*, 11271. [CrossRef]
2. Pinho, S.T.R.; Ferreira, C.P.; Esteva, L.; Barreto, F.R.; Silva, V.M.e.; Teixeira, M.G.L. Modelling the dynamics of dengue real epidemics, *Philos. Transact. R. Soci. Math. Phys. Eng. Sci.* **2010**, *368*, 5679–5693.
3. Kongnuy, R.; Pongsumpun, P. Mathematical modeling for dengue transmission with the effect of season. *Int. J. Biol. life Sci.* **2011**, *7*. Available online: <https://api.semanticscholar.org/CorpusID:53350234> (accessed on 2 October 2023).

4. Side, S.; Noorani, S.M. A SIR model for spread of dengue fever disease (simulation for South Sulawesi, Indonesia and Selangor, Malaysia). *World J. Model. Simul.* **2013**, *9*, 96–105.
5. Gakkhar, S.; Chavda, N.C. Impact of awareness on the spread of dengue infection in human population. *Appl. Math.* **2013**, *4*, 142–147. [[CrossRef](#)]
6. Hanif, A.; Butt, A.I.K. Atangana-Baleanu fractional dynamics of dengue fever with optimal control strategies. *AIMS Math.* **2023**, *8*, 15499–15535. [[CrossRef](#)]
7. Khan, M.A.; Fatmawati. Dengue infection modeling and its optimal control analysis in East Java, Indonesia. *Heliyon* **2021**, *7*, e06023. [[CrossRef](#)]
8. Fatmawati; Jan, R.; Khan, M.A.; Khan, Y.; ullah S. A new model of dengue fever in terms of fractional derivative. *Math. Biosci. Eng.* **2020**, *17*, 5267–5287. [[CrossRef](#)]
9. Rowe, D.; McDermott, C.; Veliz, Y.; Kerr, A.; Whiteside, M.; Coss, M.; Huff, C.; Leal, A.; Kopp, E.; LaCrue, A.; et al. Dengue Outbreak Response during COVID-19 Pandemic, Key Largo, Florida, USA, 2020. *Emerg. Infect. Dis.* **2023**, *29*, 1643–1647. [[CrossRef](#)]
10. Disease Outbreak News: Dengue-Bangladesh, World Health Organization Report. Available online: <https://www.who.int/emergencies/disease-outbreak-news/item/2023-DON481> (accessed on 11 August 2023).
11. Brady, O.J.; Gething, P.W.; Bhatt, S.; Messina, J.P.; Brownstein, J.S.; Hoen, A.G.; Moyes, C.L.; Farlow, A.W.; Scott, T.W.; Hay, S.I. Refining the Global Spatial Limits of Dengue Virus Transmission by Evidence-Based Consensus. *PLoS Negl. Trop. Dis.* **2012**, *6*, e1760. [[CrossRef](#)]
12. Bonyah, E.; Khan, M.A.; Okosun, K.O.; GoÂ´mez-Aguilar, J.F. On the co-infection of dengue fever and Zika virus, *Optim. Control. Appl. Methods* **2019**, *40*, 394–421. [[CrossRef](#)]
13. CDC Report. Available online: <https://www.cdc.gov/dengue/symptoms/index.html> (accessed on 20 September 2021).
14. Pongsumpun, P. Mathematical model of dengue disease with the incubation period of virus. *World Aca. Sci.Eng. Tech.* **2008**, *44*, 328–332.
15. Adom-Konadu, A.; Yankson, E.; Naandam, S.M.; Dwomoh, D. A Mathematical Model for Effective Control and Possible Eradication of Malaria. *Hindawi J. Math.* **2022**. [[CrossRef](#)]
16. Traor, B.; Sangar, B.; Traor, S. A Mathematical Model of Malaria Transmission with Structured Vector Population and Seasonality. *Hindawi J. Appl. Math.* **2017**, *2017*, 6754097. [[CrossRef](#)]
17. Al Basir, F.; Abraha, T. Mathematical Modelling and Optimal Control of Malaria Using Awareness-Based Interventions. *Mathematics* **2023**, *11*, 1687. [[CrossRef](#)]
18. World Health Organisation. Malaria. 2021. Available online: <https://www.who.int/news-room/fact-sheets/detail/malaria> (accessed on 29 March 2023).
19. Al-Arydah, M.; Smith, R. Controlling malaria with indoor residual spraying in spatially heterogenous environments. *Math. Biosci. Eng.* **2011**, *8*, 889–914. [[CrossRef](#)]
20. Selvaretnam, A.A.; Sahu, P.S.; Sahu, M.; Ambu, S. A review of concurrent infections of malaria and dengue in Asia. *Asian Pac. J. Trop.* **2016**, *6*, 633–638. [[CrossRef](#)]
21. Wiwanitkit, V. Concurrent malaria and dengue infection: A brief summary and comment. *Asian Pac. J. Trop. Biomed.* **2011**, *1*, 326–327. [[CrossRef](#)]
22. Centers for Disease Control and Prevention. *Biology*; Centers for Disease Control and Prevention: Atlanta, GA, USA, 2015. Available online: <http://www.cdc.gov/malaria/about/biology/> (26 February 2016).
23. Gautam, A.; Aryal, U.; Bhandari, S.; Pradhan, S.; Bhattarai, U.; Mishra, A.; Sharma, S.K. Dengue and malaria coinfection: The first case report in Nepal. *Oxf Med Case Rep.* **2022**, *2022*, omac022. [[CrossRef](#)]
24. Handari, B.D.; Vitra, F.; Ahya, R.; Nadya, T.; Aldila, D. Optimal control in a malaria model, intervention of fumigation and bed nets. *Adv. Differ. Equ.* **2019**, *2019*, 497. [[CrossRef](#)]
25. Sheoran, N.; Satia, M.H. Stability Analysis of Co-Infection of Malaria-Dengue. In *Mathematical Models of Infectious Diseases and Social Issues*; IGI Global: Hershey, PA, USA, 2020; pp. 138–177, ISBN13: 9781799837411. [[CrossRef](#)]
26. Butt, A.I.K.; Ahmad, W.; Rafiq, M.; Baleanu, D. Numerical analysis of Atangana-Baleanu fractional model to understand the propagation of a novel corona virus pandemic. *Alex. Eng. J.* **2022**, *61*, 7007–7027. [[CrossRef](#)]
27. Rafiq, M.; Ahmad, W.; Abbas, M.; Baleanu, D. A reliable and competitive mathematical analysis of Ebola epidemic model. *Adv. Differ. Equ.* **2020**, *2020*, 540. [[CrossRef](#)]
28. Ahmad, W.; Rafiq, M.; Abbas, M. Mathematical analysis to control the spread of Ebola virus epidemic through voluntary vaccination. *Eur. Phys. J. Plus.* **2020**, *135*, 775.
29. Ahmad, W.; Abbas, M.; Rafiq, M.; Baleanu, D. Mathematical analysis for the effect of voluntary vaccination on the propagation of Corona virus pandemic. *Results Phys.* **2021**, *31*, 104917. [[CrossRef](#)]
30. Gul, N.; Khan, S.U.; Ali, I.; Khan, F.U. Transmission dynamic of stochastic hepatitis C model by spectral collocation method. *Comput. Biomech. Biomed. Eng.* **2022**, *25*, 578–592. [[CrossRef](#)] [[PubMed](#)]
31. Ali, I.; Khan, S.U. Threshold of Stochastic SIRS Epidemic Model from Infectious to Susceptible Class with Saturated Incidence Rate Using Spectral Method. *Symmetry* **2022**, *14*, 1838. [[CrossRef](#)]
32. Butt, A.I.K.; Ahmad, W.; Rafiq, M.; Ahmad, N.; Imran, M. Optimally analyzed fractional Coronavirus model with Atangana-Baleanu derivative. *Results Phys.* **2023**, *53*, 106929, ISSN 2211-3797. [[CrossRef](#)]

33. Osman, T.; Cemil, T. Solution estimates to Caputo proportional fractional derivative delay integro-differential equations. *Rev. Real Acad. Cienc. Exactas Fisicás Nat. Ser. Matemáticas* **2023**, *117*, 12.
34. Tun, C.; Tun, O. On the Fundamental Analyses of Solutions to Nonlinear Integro-Differential Equations of the Second Order. *Mathematics* **2022**, *10*, 4235. [[CrossRef](#)]
35. Bohner, M.; Tun, O. Qualitative analysis of integro-differential equations with variable retardation. *Discret. Contin. Dyn. Syst.—B* **2022**, *27*, 639–657. [[CrossRef](#)]
36. Martchva, M. *An Introduction to Mathematical Epidemiology*; Springer Science+Business Media: New York, NY, USA, 2015.
37. Samui, P.; Mondal, J.; Khajanchi, S. A mathematical modeling of Covid-19 transmission dynamics with a case study of Wuhan. *Chaos Solitons Ractal* **2020**, *140*, 110173. [[CrossRef](#)] [[PubMed](#)]
38. Augusto, F.B. Optimal chemoprophylaxis and treatment control strategies of a tuberculosis transmission model. *World J. Model Simul.* **2009**, *5*, 163–173.
39. Butt, A.I.K.; Chamaleen, D.B.D.; Batool, S.; Nuwairan, M.A. A new design and analysis of optimal control problems arising from COVID-19 outbreak. *Math. Meth. Appl. Sci.* **2023**, *46*, 16957–16982. [[CrossRef](#)]
40. Arnold, V.I. *Ordinary Differential Equations. Translated and Edited by Richard A.Silverman*; The M.I.T. Press: Cambridge, MA, USA, 1998.
41. Kreyszig, E. *Introductory Functional Analysis with Application*; John Wiley and Sons: New York, NY, USA, 1993.
42. Castillo-Chavez, C.; Feng, Z.; Huanz, W.; Driessche, P.V.D.; Kirschner, D.E. On the computation of RO and its role in global stability. In *Mathematical Approaches for Emerging and Reemerging Infectious Diseases: An Introduction, IMA. 2002*, 125; Springer: Berlin/Heidelberg, Germany, 2002.
43. Wiggins, S. *Introduction to Applied Nonlinear Dynamical Systems and Chaos*; Princeton University Press: Princeton, Japan, 2003.
44. Van Den Driessche P. Reproduction numbers of infectious disease models. *Infect. Dis. Model.* **2017**, *2*, 288–303. [[CrossRef](#)] [[PubMed](#)]

**Disclaimer/Publisher’s Note:** The statements, opinions and data contained in all publications are solely those of the individual author(s) and contributor(s) and not of MDPI and/or the editor(s). MDPI and/or the editor(s) disclaim responsibility for any injury to people or property resulting from any ideas, methods, instructions or products referred to in the content.